Molecular Biology of the Cell
Vol. 21, 725–738, March 1, 2010

Fate Specification and Tissue-specific Cell Cycle Control of the *Caenorhabditis elegans* Intestine

Alexandra Segref,*† Juan Cabello,‡§ Caroline Clucas,*‖ Ralf Schnabel,§ and Iain L. Johnstone*

*Division of Molecular Genetics, Institute of Biomedical and Life Sciences, University of Glasgow, Glasgow G12 8QQ, United Kingdom; ‡Oncology Area, Centre for Biomedical Research of La Rioja, 26006 Logrono, Spain; and §Institut für Genetik, TU Braunschweig, 38106 Braunschweig, Germany

Submitted April 2, 2009; Revised December 18, 2009; Accepted December 24, 2009
Monitoring Editor: Marcos Gonzalez-Gaitan

Coordination between cell fate specification and cell cycle control in multicellular organisms is essential to regulate cell numbers in tissues and organs during development, and its failure may lead to oncogenesis. In mammalian cells, as part of a general cell cycle checkpoint mechanism, the F-box protein β-transducin repeat-containing protein (β-TrCP) and the Skp1/Cul1/F-box complex control the periodic cell cycle fluctuations in abundance of the CDC25A and B phosphatases. Here, we find that the *Caenorhabditis elegans* β-TrCP orthologue LIN-23 regulates a progressive decline of CDC-25.1 abundance over several embryonic cell cycles and specifies cell number of one tissue, the embryonic intestine. The negative regulation of CDC-25.1 abundance by LIN-23 may be developmentally controlled because CDC-25.1 accumulates over time within the developing germline, where LIN-23 is also present. Concurrent with the destabilization of CDC-25.1, LIN-23 displays a spatially dynamic behavior in the embryo, periodically entering a nuclear compartment where CDC-25.1 is abundant.

INTRODUCTION

Integration of developmental fate specification and control of the eukaryotic cell cycle is essential to regulate cell number in tissues and organs. The eukaryotic cell cycle is driven by cyclin-dependent kinases, whose activation requires the removal of inhibitory phosphates by Cdc25 phosphatases (Boutros *et al*., 2006). We described previously an intestinal-specific hyperplasia of *Caenorhabditis elegans* caused by *cdc-25.1(ij48)*, a gain-of-function mutation causing the amino acid substitution CDC-25.1(S46F), where S46 is within a putative aspartic acid-serine-glycine (DSG) phosphorylation site that is also a consensus glycogen synthase kinase (GSK)3β phosphorylation site (Clucas *et al*., 2002). A similar mutant CDC-25.1(G47D) was identified independently of our study (Kostic and Roy, 2002). Because CDC-25.1 function is required in probably all early *C. elegans* cell types to drive normal proliferation (Ashcroft *et al*., 1999; Clucas *et al*., 2002), the intestinal-specific phenotype of these mutants suggests interplay between intestinal fate specification and cell cycle control regulated by CDC25.1.

This article was published online ahead of print in *MBC in Press* (http://www.molbiolcell.org/cgi/doi/10.1091/mbc.E09–04–0268) on January 6, 2010.

Present addresses: † Cologne Excellence Cluster on Cellular Stress Responses in Aging-associated Diseases (CECAD) at the Institute for Genetics, University of Cologne, Cologne, Germany; ‖ University of Glasgow, The Wellcome Centre for Molecular Parasitology, Glasgow Biomedical Research Centre, 120 University Place, Glasgow G12 8TA, Scotland, United Kingdom.

Address correspondence to: Iain L. Johnstone (i.johnstone@bio.gla.ac.uk).

In cultured mammalian cells, ubiquitin-mediated proteolysis by the F-box protein β-transducin repeat-containing protein (β-TrCP), a component of the Skp1/Cul1/F-box (SCF) ubiquitin ligase, has been shown to control the periodic cell cycle fluctuations and DNA damage response through abundance of CDC25A and B via DSG and aspartic acid-aspartic acid-glycine (DDG) motifs, respectively (Busino *et al*., 2003; Jin *et al*., 2003). Also, elevated CDC25A/B protein levels have been detected in many human malignancies (Kristjansdottir and Rudolph, 2004). A similar regulatory process exists in the Wnt pathway where the adenomatous polyposis coli (APC)/Axin/GSK3β destruction-box complex phosphorylates the DSG motif of human β-catenin, promoting its β-TrCP–dependent ubiquitination and proteasomal degradation (Kikuchi *et al*., 2006). Mutations in either *APC* or the β-catenin DSG motif cause stabilization of β-catenin and are associated with human intestinal hyperplasia and oncogenesis (Polakis, 2000; Ougolkov *et al*., 2004; Gregorieff and Clevers, 2005). Therefore, we tested whether the intestinal hyperplasia caused by the *C. elegans* CDC-25.1(S46F) DSG mutant was the result of an abrogation of its β-TrCP or APC/GSK3β-dependent regulation.

The *C. elegans* intestine consists of 20 cells derived from a single founder cell termed E (Sulston *et al*., 1983). The parental cell of E is the pluripotent EMS blastomere, and its division is considered a binary decision between two developmental fates, its anterior daughter-cell MS (mesoderm) and posterior daughter-cell E (endoderm/intestine). This pluripotent capacity of EMS is sometimes described as mesendoderm. Specification of E as endoderm depends on a Wnt signal from the P_2 blastomere. Isolation of EMS from the P_2-derived Wnt signal causes two MS-like daughters to be born (Goldstein, 1993, 1995) and mutations that block the Wnt pathway cause the same E-to-MS fate transformation (Rocheleau *et al*., 1997, 1999; Thorpe *et al*., 1997; Schlesinger *et al*., 1999; Maduro *et al*., 2001; Bei *et al*., 2002). In the

canonical Wnt pathway that regulates human intestinal development, Wnt-activated Frizzled causes negative regulation of GSK3β, resulting in stabilization of β-catenin; hence, loss of GSK3β activity would mimic constitutive activation of the Wnt signal and have an opposite phenotype to loss of positive-acting pathway members (Kikuchi *et al*., 2006). However, during endodermal fate specification in *C. elegans*, interference of *gsk-3* (GSK3β) has been interpreted as causing the same phenotype as loss of positive-acting Wnt members. To explain this enigma, in this one case GSK3 has been proposed to be activated in response to reception of the Wnt signal, although no known molecular mechanisms or biochemical data exist to support this hypothesis (Korswagen, 2002). Among the outcomes of endodermal fate specification is a change in the regulation of the cell cycle. The intestinal cells have a significantly longer cell cycle to those of the sister MS lineage and to most other early embryonic lineages. This is believed to be the result of the inclusion of a Gap phase in the intestinal lineage (Edgar and McGhee, 1988).

We find the *C. elegans* β-TrCP orthologue LIN-23 regulates CDC-25.1 abundance negatively in all early embryonic tissues; the negative regulation of CDC-25.1 by LIN-23 in the embryo was also concluded from a recent genetic analysis (Hebeisen and Roy, 2008). Although CDC-25.1 is destabilized by LIN-23 in most or all early embryonic tissues, we find those cells specified as intestine, either by normal development or ectopically, are particularly sensitive to failure of this down-regulation. In addition to causing the intestinal hyperplasia, interference of *lin-23* function in the embryo significantly shortens the long intestinal cell cycle but does not shorten the already short MS lineage cell cycle. By investigating cell lineage defects caused by *gsk-3(RNAi)*, we were able to show that long intestinal cell cycles created ectopically by the transformation of another cell lineage by *gsk-3(RNAi)* were equally sensitive to cell cycle shortening by stabilization of CDC-25.1 as those of the normal intestinal lineage. We conclude that endodermal fate specification and not lineage of descent must determine the switch to the long, Gap phase-containing cell cycles of the *C. elegans* intestine and their concomitant switch to sensitivity to LIN-23–dependent regulation of CDC-25.1. This regulatory mechanism is therefore a significant rate-limiting step in the long intestinal cell cycles but not in the majority of other short embryonic cell cycles such as those of the MS lineage.

We find evidence that the regulation of CDC-25.1 by LIN-23 is developmentally controlled. Here, we demonstrate that *lin-23* acts as a maternal gene with respect to its embryonic functions including the degradation of CDC-25.1; we demonstrated previously that *cdc-25.1* is also maternal for embryonic function (Clucas *et al*., 2002). In this study, we show that both LIN-23 and CDC-25.1 proteins are present in the maternal germline and that at the time of fertilization the oocyte contains both proteins maternally derived. Although maternally derived LIN-23 promotes the rapid decline in abundance of maternally derived CDC-25.1 in probably all cells of the early embryo, within the maternal germline CDC-25.1 accumulates in the presence of LIN-23. Finally, we find that the subcellular localization of LIN-23 becomes dynamic in the early embryo concurrent with the onset of CDC-25.1 destabilization, where we detect its periodic localization to the nucleus. Because LIN-23 seems to be excluded from nuclei within the germline, it is interesting to speculate whether its periodic nuclear localization in the early embryo is related to its destabilization of CDC-25.1, which is predominantly nuclear localized in the cells of the early embryo.

MATERIALS AND METHODS

C. elegans Strains

C. elegans strains used in this study were N2 Bristol, JR1838 *wIs84*[pJM66 *elt-2::GFP::LacZ*, pRF4 *rol-6(su1006dm)*] (intestinal green fluorescent protein [GFP]), IA105 *unc-76(e911)V; ijIs12[dpy-7::GFP::lacZ, unc-76(+)]* (hypodermal GFP), JR667 *unc-119(e2498::Tc1)III; wIs51[pMF1, pDP#MM016B unc-119(+)]* (seam cell GFP), IA522 *unc-76(e911)V*; *ijEx31[elt-2::LAP::cdc-25.1, p76-16B unc-76(+)]*, IA530 *cdc-25.1(ij48)I*; *wIs84*, IA535 *ijIs16[elt-2::LAP::cdc-25.1, p76-16B unc-76(+)]*, IA565 *lin-23(e1883)/+II; wIs119*[pDP#MM016B *unc-119(+)*, pMW025 (*npa-1::GFP::LacZ)*], IA568 *lin-23(e1883)/+I; wIs84*, IA582 *unc-119(ed3)III; ijIs18 [lin-23::FLAG-TY, unc-119(+)]*, IA589 *lin-23(e1883)II; unc-119(ed3)III; ijIs18 [lin-23::FLAG-TY, unc-119(+)]*, IA592 *lin-23(e1883)II; ijIs18 [lin-23::FLAG-TY, unc-119(+)]; wIs84*, IA593 *cdc-25.1(ij48)I; lin-23(e1883)II; ijIs18[lin-23::FLAG-TY, unc-119(+)]; wIs84*. CB3514 *lin-23(e1883)/dpy-10(e128)II* and DP38 *unc-119(ed3)* were obtained from the *C. elegans* Genetics Stock Center (University of Minnesota, Twin Cities, MN), which is funded by the National Institutes of Health National Center for Research Resources. JR1838 and JR667 were kindly supplied by Joel Rothman (Department of Molecular, Cellular, and Developmental Biology, University of California, Santa Barbara, Santa Barbara, CA).

Plasmid Constructs

The plasmid pAS10 (pBS-*unc119-lin-23::FLAG-TY*) contains a FLAG-tagged and TY epitope-tagged transgene of *lin-23* fused to upstream sequences of *lin-23* necessary for its expression, plus a copy of the *unc-119* gene that is used for selection of integrative transgenesis. pAS11 (pGEX6P-*lin-23*) is a *GST::lin-23* cDNA expression clone, and pAS5 (pQE30-*cdc-25.1*) is a HIS_6*::cdc-25.1* cDNA clone used for recombinant LIN-23 or CDC-25.1 protein synthesis.

Genomic *lin-23* was cloned using the oligonucleotides (oligos) 5′-GGTACCCCAAATTTGCCTCTGATTCCG and 5′-GGTACCGTTGCAGAAAT GCTCAAATCGG to clone 2183 base pairs of upstream promoter, the complete *lin-23* gene, and 766-base pair 3′ untranslated region (UTR) into the KpnI site of pBS-SK (Stratagene, La Jolla, CA) to generate pAS7 (pBS-*lin-23*). For *lin-23::FLAG-TY*, the following oligos were used to insert the FLAG and TY tag in frame at the 3′ end of the *lin-23* genomic DNA as BamHI, SpeI fragments using oligos 5′-ACTAGTCTTGTCGTCGTCATCCTTGTAGTCTGGGCCACCATCTGGCATCTCTTC, 5′-ACTAGTGAGGTCCATACTAACCAGGACCCACTTGACTAAAATCTACACTCCTTCCCATTTT, and 5′CGACGAGGAATTGCATGTCTTC and M13rev and cloned into pAS7 cut with BamHI to generate pAS8 (pBS-*lin-23::FLAG-TY*). A 5.7-kb *unc-119* gene XbaI/HindIII cassette was cloned as XbaI/HindIII cassette into pBS-SK and the *lin-23::FLAG-TY* subsequently inserted as a KpnI fragment to generate pAS10 (pBS-*unc-119-lin-23::FLAG-TY*). *GST::lin-23* was cloned by amplification of the *lin-23* cDNA by using oligos 5′-CCCGGGTTCTTCACCGCACCGAGCTTCAAC and 5′-CCCGGGTTATGGGCCACCATCTGGCATCTC and insertion as SmaI fragment into pGEX6P1 (GE Healthcare, Little Chalfont, Buckinghamshire, United Kingdom) to generate pAS11 (pGEX6P-*lin-23*). A 797-base pair BamHI *lin-23* cDNA fragment was cloned into pQE80L (QIAGEN, Dorking, Surrey, United Kingdom) to generate HIS_6*::lin-23*-C-terminus [pAS14 (pQE80L-*lin-23-C*)]. 5′-GGATCCGCTACCACCGGGGAAAAAGC and 5′-GAGCTCTTATTCGGCGTCGTCAGAAAT oligos were used to clone *cdc-25.1* cDNA as BamHI/SacI fragment into pQE30 (QIAGEN) to generate HIS_6*::cdc-25.1* [pAS5 (pQE30-*cdc-25.1*)].

The plasmid pAS1 (pBS-*elt-2::LAP::cdc-25.1*) contains an LAP (GFP-S-tag-TEV cleavage site) tagged *cdc-25.1* transgene fused to the *elt-2* promoter.

The 5068-base pair *elt-2* promoter fragment was amplified by polymerase chain reaction (PCR) with the oligos 5′-TTTTCTCGAGCGAGCTGAATACACGTGCT and 5′-TTTTGGATCCTCTATAATCTATTTTCTAGTTTC (from the pJM69 vector; a gift from J. McGhee, University of Calgary, Calgary, AB, Canada). PCR amplification of a 2569-base pair *cdc-25.1* genomic DNA fragment was done using the oligos 5′-TTTTGGATCCGCTACCACCGGGGAAAAAGC and 5′-TTTTTCTAGAGCTGAGATTAATGTGAACGC; this fragment starts at the first codon following the *cdc-25.1* ATG and includes 478 base pairs of 3′ UTR. The fragments were cut with XhoI/BamHI (*elt-2*) and BamHI/XbaI (*cdc-25.1*) and inserted into pBS-SK that was digested with XhoI and XbaI. The resulting vector was subsequently digested with BamHI and the LAP tag (GFP-S-tag-TEV cleavage site) inserted in frame as a 1086-base pair BamHI fragment that was derived from BamHI digestion of the pIC26 vector (a gift from I. Cheeseman, Whitehead Institute for Biomedical Research, Cambridge, MA).

Chromosomal Integration of Extrachromosomal Transgenes

By a standard procedure, IA522 animals were irradiated with 3800 rad by using a ^{60}Co source to integrate the extrachromosomal array *ijEx31[elt-2::LAP::cdc-25.1, p76-16B unc-76(+)]*, selecting for *unc-76* rescued worms. This generated several stably integrated lines. One line was selected for use and backcrossed four times against N2 to remove potential and unwanted mutations, generating the strain IA535.

Microparticle Bombardment

Integration of *lin-23::FLAG-TY* was done by microparticle bombardment of DP38 *unc-119(ed3)* essentially as described by Praitis *et al*. (2001), using NotI

linearized pAS10. NonUnc larvae were selected and several strains were analyzed for germline expression of LIN-23::FLAG-TY. One strain that displayed expression of tagged LIN-23::FLAG-TY protein in the germline was selected for further analysis to generate IA589, IA592, and IA593.

RNA Interference (RNAi)

C. elegans GSK3β genes were identified from the literature (Schlesinger *et al*., 1999) and by BLAST searches. The genes selected were *gsk-3* (Y18D10A.5), which is probably orthologous and C44H4.6, a GSK3 family member. *lin-23* is orthologous to human β-TrCP and *sel-10* is the next most closely related (Kipreos *et al*., 2000). The *C. elegans* cullins, *pop-1*, and *apr-1* were all identified from the literature (Kipreos *et al*., 1996; Rocheleau *et al*., 1997). The following genomic fragments (relative to the genomic ATG) were cloned into the pPD129.36 vector: *lin-23* (K10B2.1), 685-1811 base pairs* and 1812-2686 base pairs; *gsk-3* (Y18D10A.5), 1266-2940 base pairs; *cullin-1* (D2045.6), 238-1234 base pairs*; *cullin-2* (ZK5204), 1990-3100 base pairs; *sel-10* (F55B12.3), 796-3010 base pairs*; *pop-1* (W10C8.2), 5171-6847 base pairs*; *apr-1* (K04G2.8), 2696-4615 base pairs; and C44H4.6, 1319-3018 base pairs. The clones indicated with an asterisk were obtained from the RNAi library (Kamath and Ahringer, 2003). For *apr-1(RNAi)*, the *apr-1* clone was in vitro transcribed to generate double-stranded RNA for microinjection. Other clones were used for bacterial feeding RNAi by using established procedures (Fraser *et al*., 2000; Timmons *et al*., 2001). Where RNAi was performed in liquid culture, RNAi bacterial strains were grown overnight in Luria-Bertani (LB) medium containing 100 μg/ml ampicillin at 37°C. The cultures were then diluted to an OD_{600} of 0.6 in a final volume of 500 ml of LB containing 100 μg/ml ampicillin and 1 mM isopropyl β-D-thiogalactoside (IPTG) and double-stranded RNA induced at 37°C for 4 h. The cultures were spun down at 4000 × *g* for 10 min, and the bacterial pellets were used to inoculate 250 ml of S-medium containing 50 μg/ml ampicillin and 0.2 mM IPTG. Starved L1-staged hermaphrodites were added to 250 ml of *lin-23*, *gsk-3*, or control RNAi S-medium and incubated for 3 d at 25°C. For *lin-23* or *sel-10*, RNAi, embryos were applied to RNAi plates, grown to adulthood at 25°C, and the phenotype was observed in their offspring. L4 hermaphrodites were fed for 24 h in *pop-1* and *cul-2* RNAi or for 48 h for *gsk-3* and *cul-1* RNAi at 25°C, and their offspring analyzed for intestinal phenotypes. RNAi of *apr-1* was performed by microinjection of in vitro-transcribed double-stranded 1919-base pair *apr-1* RNA into young adult hermaphrodites, and the phenotype was observed after incubation at 20°C for 24 h. Typically, ~12% of all (40% of RNAi-arrested) embryos displayed intestinal hyperplasia. RNAi was performed in *C. elegans* liquid culture for subsequent protein extraction from embryos. Embryos were collected using the standard bleach method (Sulston and Hodgkin, 1988), lysed in lysis buffer (see Immunoprecipitation), and equal amounts of total protein were resuspended in sample buffer and applied to SDS-polyacrylamide gel electrophoresis (PAGE) followed by Western blotting.

Antibodies

Antibodies were raised against recombinant LIN-23 and CDC-25.1. The plasmid clones used were pAS5 (pQE 30-*cdc-25.1*) and pAS11 (pGEX6P-*lin-23*).

pAS5 was constructed by amplifying by PCR a 1815-base pair cDNA sequence of *cdc-25.1* with the oligonucleotides 5′-TTTTGGATCCGCTACCACCGGGGAAAAAGC-3′ and 5′-TTTTGAGCTCTTATTCGGCGTCGTCAGAAAT-3′. After restriction digestion with BamHI and SacI, the fragment was cloned into pQE30. A 1995-base pair *lin-23* cDNA fragment (lacking the endogenous ATG) was PCR amplified using the oligonucleotides 5′-TTTTCCCGGGTTCTTCACCGCACCGAGCTTCAAC-3′ and 5′-TTTTCCCGGGTTATGGGCCACCATCTGGCATCTC-3′. The amplified fragment was digested with SmaI and inserted in frame into the SmaI site of pGEX-6P-1. The HIS_6::CDC-25.1 and GST::LIN-23 proteins were used to immunize rabbits (SNBTS, Scotland). For affinity purification of antibodies, the recombinant proteins in 4 M urea and 0.1 M sodium borate, pH 8.3, were cross-linked to activated CNBr-Sepharose (GE Healthcare) according to manufacturer's instructions. Each rabbit serum, diluted in an equal volume of phosphate-buffered saline (PBS) was incubated overnight at 4°C with the appropriate recombinant protein cross-linked to CNBr-Sepharose. The beads were subsequently poured into a 10-ml Poly-Prep column (Bio-Rad Laboratories, Hemel Hempstead, United Kingdom), and the flow-through was collected. The antibody, bound to the beads, was washed once with 10 ml of wash buffer (1× PBS-Tween 20 at 0.1%), followed by three washes with 10 ml of 1× PBS. Bound antibodies were eluted with 10 ml of elution buffer (100 mM glycine and 200 mM NaCl, pH 2.2), and 1-ml fractions were collected on ice in 1.5-ml microcentrifuge tubes containing 200 μl of 1 M Tris, pH 8.0, to neutralize the acidic pH from the elution buffer. The OD_{280} of all fractions were measured, and those with the highest antibody concentrations were pooled. Antibodies were precipitated with 50% ammonium sulfate, suspended in PBS-Glycerol (PBS-G), and further dialyzed against 1× PBS-G at 8.7% for 10 h at 4°C. Anti-CDC-25.1 peptide antibodies used for immunostaining or Western blotting were as described previously (Clucas *et al*., 2002).

Immunoprecipitation and Western Blotting

Immunoprecipitation from embryonic extracts or L4-stage hermaphrodites was essentially done as described in Desai *et al*. (2003), with slight modifications. In brief, for embryonic extracts, *C. elegans* L1 larvae were grown in large-scale liquid S-medium cultures to adulthood. Embryos were collected using the standard bleach method (Sulston and Hodgkin, 1988) and suspended in lysis buffer (50 mM Tris, pH 7.5, 100 mM KCl, 1 mM EDTA, 1 mM $MgCl_2$, 8.7% glycerol, 0.05% NP-40, 1× Protease Inhibitor Cocktail [Roche Diagnostics, Mannheim, Germany], and 1× Phosphatase Inhibitor Cocktail I and II [Sigma Chemical, Poole, Dorset, United Kingdom]), quickly frozen in liquid nitrogen, and lysed by sonication using an Ultrasonic processor with 5-mm microtip (Jencons, Leyton Buzzard, United Kingdom) for 10 pulses over 10 s at 30% amplitude. Where L4-stage hermaphrodites were used, L1 worms were grown as described above, and worms were collected before they reached adulthood at the early to late L4 stage and lysed in lysis buffer (as performed for embryos). After sonication, extracts were precleared by centrifugation at 30,000 × *g* for 20 min at 4°C. The precleared extract (300 μg of total protein) was incubated with 40 μg of anti-CDC-25.1 affinity-purified antibody (this study) cross-linked to protein A-agarose (Bio-Rad Laboratories), or as control, a similar amount of rabbit immunoglobulin (Ig)G (Sigma Chemical) cross-linked to protein A-agarose was used in a total volume of 200 μl of lysis buffer containing 1% NP-40, the inclusion of which reduced nonspecific binding of proteins to the matrix. The samples were rotated for 1 h at 4°C, the beads were washed three times with lysis buffer, and eluted with 30 μl of glycine/HCl and 200 mM NaCl, pH 2.2. After immunoprecipitation, eluates were diluted in 30 μl of SDS sample buffer, heated to 95°C for 4 min, and typically 3% of total for input and 30% for the eluates were applied to SDS-PAGE followed by Western blotting with anti-CDC-25.1 (1:400; Clucas *et al*., 2002), anti-LIN-23 (1:750), anti-ubiquitin (1:1000; Covance Research Products, Princeton, NJ), anti-GSK3β (1:500; Sigma Chemical), or anti-β-actin (1:2000; Sigma Chemical) antibodies. Where extracts were not subjected to immunoprecipitation (see Figures 2, A and B, and 3B), the same amount of total protein derived from those extracts was resuspended in SDS sample buffer, heated to 95°C as described above, and then directly applied to SDS-PAGE and analyzed by Western blotting. In Figure 5, worms were first collected in 1× M9 buffer, resuspended in SDS sample buffer, heated at 95°C, and applied to SDS-PAGE analysis followed by Western blotting.

Purification of LAP::CDC-25.1 on S-Protein Agarose

Embryos were prepared as described under Immunoprecipitation. Embryos were lysed in lysis buffer (50 mM Tris, pH 7.5, 300 mM KCl, 1 mM EDTA, 0.05% NP-40, 1× Protease Inhibitor Cocktail [Roche Diagnostics], and 1× Phosphatase Inhibitor Cocktail I and II (Sigma Chemical). Sixty micrograms of S-protein agarose (Novagen, Madison, WI) was washed once with 400 μl of lysis buffer. Three hundred micrograms of total protein in lysis buffer was incubated with the washed S-protein agarose in a total volume of 200 μl; 10 μl was kept aside as input control. The mixture was incubated in a 1.5-ml microcentrifuge tube for 3 h at 4°C with continuous end-over-end rotation, the flow-through was collected, and the beads were washed three times with 400 μl of lysis buffer. The samples were eluted for 3 min at room temperature in 60 μl of SDS sample buffer followed by 4-min incubation at 95°C. A fraction of the input and flow-through was suspended in equal volume of SDS sample buffer and boiled at 95°C for 4 min. Five microliters of the input and flow-through and 20 μl of the eluate were applied to 10% SDS-PAGE to probe with anti-GFP or anti-LIN-23 antibodies.

Conventional Microscopy for Live Imaging

Live imaging was performed according to Sulston and Hodgkin (1988) by using an Axioplan 2 microscope (Carl Zeiss, Jena, Germany) equipped with Nomarski optics using the 63×/1.4 Plan-Apochromat lens. GFP fluorescence was viewed using a tungsten halogen lamp UV source at 488 nm. Images were taken with a C4742-95 digital camera (Hamamatsu Photonic, Hamamatsu City, Japan) and Openlab 4.0.2. software (Improvision, Coventry, United Kingdom). Images were processed using Photoshop 8.0 and Illustrator 12 (Adobe Systems, Mountain View, CA) for figure assembly.

Cell Lineage Analysis

Four-dimensional microscopy for cell lineage analysis was as described in Schnabel *et al*. (1997). Lineages are derived from embryos cultured at 25°C. RNAi was performed by the bacterial feeding method as described above. The *C. elegans* strains used were JR1838 and IA530.

Immunocytochemistry

Immunostaining of CDC-25.1 was performed as described previously (Clucas *et al*., 2002), with the exception that anti-CDC-25.1 peptide antibody was used at 1:150 dilution and embryos were analyzed using an LSM 510 META confocal microscope (Carl Zeiss) at 405 nm and 543 nm for 4,6-diamidino-2-phenylindole (DAPI; Vector Laboratories, Burlingame, CA) and Alexa Fluor 594 (Invitrogen, Paisley, United Kingdom), respectively. Samples were examined using 63×/1.4 Plan Apochromat lens and 2× optical zoom. Typical settings for nonstacked images were 1012 frame size, line-step: 1, maximum scan speed, 12 bit data depth, scan direction: single, mode: line, method: mean

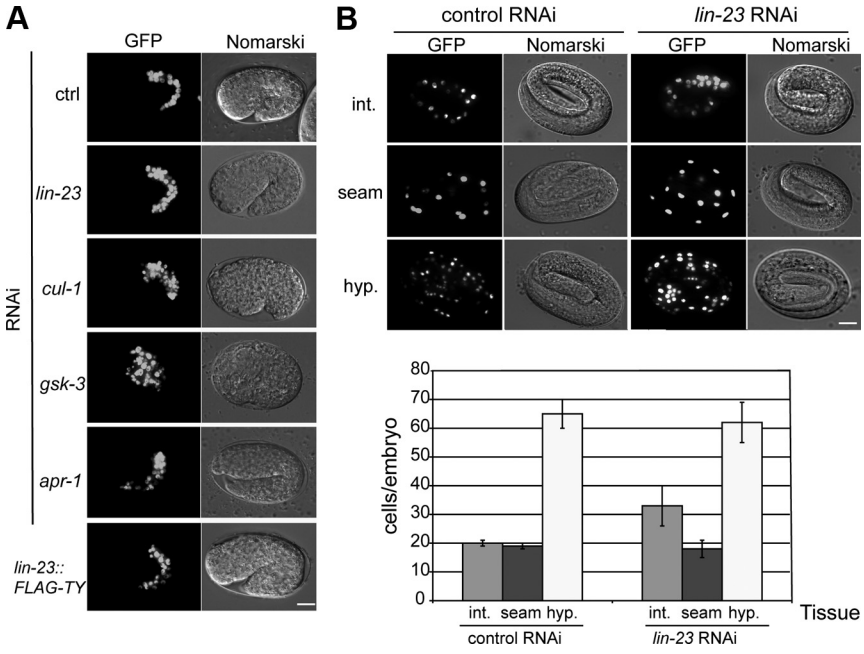

Figure 1. *C. elegans* excess endoderm phenotypes. (A) Left, GFP fluorescence of JR1838 carrying the *elt-2::GFP* transgene at the comma stage or in early arrested embryos after control (ctrl), *lin-23*, *cul-1*, *gsk-3*, or *apr-1* RNAi or in IA592 *lin-23::FLAG-TY* (see *Materials and Methods* for genotype). Right, corresponding Nomarski counterparts. Bar, 10 μm. (B) *lin-23(RNAi)* triggers predominantly hyperplasia of the intestine under mild RNAi conditions. Top, phenotypes of strain JR1838 carrying *elt-2::GFP* (int.), JR667 *wIs51* carrying a seam cell GFP reporter (seam), and IA105 carrying the hypodermal reporter *dpy-7::GFP* (hyp.) in control or *lin-23(RNAi)* embryos at the threefold stage. Bar, 10 μm. Bottom, quantification of GFP-positive cells (mean ± SD, number of embryos from two independent experiments in parentheses): intestinal cells (int.): control, 20.0 ± 1.0 (40); *lin-23(RNAi)*, 32.7 ± 6.8 (58); seam cells: control, 19.4 ± 1.2 (81) and *lin-23(RNAi)*, 18.3 ± 2.8 (79); and hypodermal cells (hyp.): control, 65.3 ± 4.6 (42) and *lin-23(RNAi)*, 62.3 ± 7.4 (45).

with average between 2 and 8 numbers. Images were taken using LSM 510 Meta version 3.2.SP2 imaging software (Carl Zeiss). Identical settings were used for comparative imaging of wild-type (WT) and mutant or control and RNAi-treated embryos at each developmental stage according to the manufacturer's instructions. The developmental stages were determined by counting the number of nuclei per embryo as revealed through DAPI staining. Due to the fast decay of CDC-25.1 from early-to-late stages of embryogenesis, the detector gain was adjusted accordingly to keep the linearity of the signal. For fluorescence quantification, the embryo was selected using LSM 510 software, the signal was extracted, and the average values of fluorescence intensities were compared. All images were processed with equivalent settings for figure assembly using Photoshop 8.0 (Adobe Systems).

In LIN-23 immunostaining, the anti-LIN-23 antibody was diluted 1:600 followed by Alexa Fluor 594. Samples were viewed at 543 nm (Alexa Fluor 594) or 405 nm (DAPI) using an Axioplan 2 microscope (Carl Zeiss), and images were obtained as described under Conventional Microscopy for Live Imaging.

Statistics

The fluorescence intensity of anti-CDC-25.1–immunostained embryos was measured as described above and analyzed using standard statistical techniques (Sokal and Rohlf, 2000; Supplemental Table 2).

RESULTS

C. elegans SCF$^{\beta\text{-}TrCP}$ Complex Members Regulate Intestinal Cell Number via CDC-25.1

We hypothesized the intestinal hyperplasia caused by the CDC-25.1(S46F) mutant might be by escape from negative regulation and predicted RNAi knockdown of component regulators might mimic its phenotype. We tested by RNAi members of the SCF$^{\beta\text{-}TrCP}$ and APC/Axin/GSK3β complexes. Previously, null mutants of the *C. elegans* β-TrCP and CUL1 orthologues *lin-23* and *cul-1* were shown to cause hyperplasia of several postembryonic tissues, but no embryonic intestinal cell proliferation defects were reported (Kipreos *et al*., 1996, 2000); however, maternal products of these may persist in null-mutant embryos. RNAi can knockdown both maternal and zygotic gene function (Fire *et al*., 1998) in *C. elegans*, and we found that *lin-23* or *cul-1* RNAi generated a hyperplasia of the intestine during embryogenesis (Figure 1A and Table 1A). To test genetically whether *lin-23* and *cul-1* function through CDC-25.1 S46, we repeated the RNAi in a *cdc-25.1(ij48)* mutant; no synergism was detected (Table 1A). Because these are nonadditive, we conclude it most likely that *lin-23* and *cul-1* function through CDC-25.1 S46 to regulate intestinal cell number. A similar interpretation of the *lin-23*–dependent regulation of CDC-25.1 controlling intestinal cell proliferation in the developing *C. elegans* embryo has been reported previously (Hebeisen and Roy, 2008).

We obtained additional corroborating data from the behavior of a *lin-23* transgene. We generated a *lin-23::FLAG-TY (ijIs18)* chromosomally integrated transgene for use in a biochemical analysis of the interaction between CDC-25.1 and LIN-23 (see below). The original strain IA582 is homozygous for the wild-type *lin-23* allele at its native chromosomal locus and for the genetically unlinked chromosomal integration of the epitope-tagged *lin-23::FLAG-TY* transgene; thus, both wild-type and epitope-tagged LIN-23 are present. This strain is healthy with no detectable lethality; thus, the site of integration does not interrupt an essential gene, and the LIN-23::FLAG-TY protein does not have a noticeable negative effect on wild-type LIN-23 function. To generate a strain in which the only LIN-23 function was of the *lin-23::FLAG-TY* transgene, we crossed the transgene into a strain with the chromosomal allele *lin-23(e1883)*, a strong loss of function and presumed null (Kipreos *et al*., 2000). The resulting strains that are homozygous for *lin-23(e1883)* and *ijIs18* display a variably penetrant lethality where ~75% of animals die during embryogenesis (see below). Animals homozygous for *lin-23(e1883)* proceed through embryogenesis normally but then display excess cell proliferation in various postembryonic cell lineages and develop as sterile adults. Thus, *lin-23(e1883)* homozygotes are derived from heterozygous mothers and as we demonstrate below, have some maternally supplied *lin-23* function. Because in *C. elegans* RNAi can target both zygotic and maternal gene function, where maternal gene function exists, RNAi can generate embryonic phenotypes that are not seen in homozygous mutants. In addition to the embryonic hyperplasia discussed above, we find *lin-23 RNAi* also causes embryonic lethality; when performed by the bacterial feeding method, ~25% of the resulting embryos

Table 1. Quantification of intestinal cells through expression of *elt-2::GFP* reporter

A

RNAi	Wild type	*cdc-25.1(ij48)*	p value	-Fold increase	% Hatch (wild type/*ij48)*
Control 25°C	20 ± 1 (n = 176/6)	24 ± 4 (n = 298/6)	<0.001	1.2	98.8 ± 0.498.4 ± 1.5
Control 20°C	19.7 ± 0.6 (n = 22/1)	29.5 ± 3.2 (n = 60/1)	<0.001	1.5	n.d.
pop-1	42 ± 8 (n = 175/3)	50 ± 11 (n = 152/3)	<0.001	1.2	<1<1
lin-23	37 ± 8 (n = 154/4)	36 ± 7 (n = 156/4)	n.s.	1.0	73.2 ± 10.869.8 ± 13.2
cul-1	33 ± 5 (n = 129/2)	33 ± 5 (n = 134/2)	n.s.	1.0	56.0 ± 4.244.7 ± 20.1
# *gsk-3*	28 ± 6 (n = 176/3)	35 ± 9 (n = 187/3)	<0.001	1.3	27.2 ± 5.420.8 ± 10.2
# *apr-1*	27 ± 5 (n = 47/3)	35 ± 6 (n = 76/3)	<0.001	1.3	n.d.[a]

B

lin-23(e1883)II	*cdc-25.1 (ij48)I*	p value	-Fold increase
ijIs18 [lin-23::FLAG-TY]	*lin-23(e1883)II ijIs18 [lin-23::FLAG-TY]*		
35 ± 9 (n = 62)	38 ± 8 (n = 69)	<0.01	1.1

Data are expressed as mean ± SD. p value, two-tailed Student's *t* test; n.s. $p > 0.05$; in parentheses, n is number of embryos expressing *elt-2::GFP*/number of independent RNAi experiments (for A). n.d., not determined. RNAi for control, *pop-1*, *lin-23*, *cul-1*, and *gsk-3* RNAi were by bacterial feeding and performed at 25°C. At this temperature, the *cdc-25.1(ij48)* allele shows a weaker phenotype than at 20°C and hence fewer extraintestinal cells. # RNAi-produced embryos of three classes of phenotypes: loss of *elt-2::GFP* expression (see text), embryos expressing *elt-2::GFP* in <20 cells, and embryos expressing *elt-2::GFP* in >20 cells (excess endoderm); only embryos with excess endoderm phenotype were counted.

[a] RNAi was performed by microinjection, yielding to low sample size, embryos with excess endoderm phenotype usually arrest before the threefold stage, loss of E fate was used as internal control for RNAi efficiency (17 and 16% for WT and IA530, respectively, in these experiments).

die (Supplemental Table S1). We conclude that the lethality seen for strains homozygous for *lin-23(e1883)* and *ijIs18* is the result of inadequate maternal *lin-23* function. Those that survive grow to adulthood and are fertile. As the lethality is fully complemented by the chromosomal wild-type *lin-23* allele, we conclude that the *lin-23::FLAG-TY (ijIs18)* allele is only partially functional in the developing embryo. Of significance, strains that are homozygous for *lin-23(e1883)* and *ijIs18* also display embryonic intestinal hyperplasia (Figure 1A). This is slightly less severe in cell number than the mean for *lin-23(RNAi)* (Table 1, A and B), but in combination with *cdc-25.1(ij48*) is indistinguishable from that of *lin-23(RNAi)* alone (Table 1, A and B). Therefore, *lin-23::FLAG-TY (ijIs18)* is only partially functional with respect both to regulation of *cdc-25.1* and in supporting embryonic viability. It behaves like a hypomorphic allele with respect to its maternal function. As a control, we used *pop-1(RNAi)*. In *pop-1* mutants, both the E blastomere and its sister cell MS adopt the intestinal fate (Lin *et al*., 1998), thus generating additional intestinal cells by an entirely different mechanism to *cdc-25.1(ij48)*. In combination, *pop-1(RNAi)* and the *cdc-25.1(ij48)* mutation are, as expected, synergistic (Table 1A).

To test tissue specificity of the *lin-23(RNAi)* effect on embryonic cell proliferation, we performed *lin-23(RNAi)* in the *C. elegans* strains JR667 and IA105, which carry a seam cell and hypodermal GFP markers, respectively. Under the conditions that caused intestinal hyperplasia, no increased proliferation of these other cell types was detected (Figure 1B and Supplemental Table S1). We conclude that during embryonic development in *C. elegans*, the intestinal cells are particularly sensitive to the perturbation of LIN-23–mediated regulation of CDC-25.1.

GSK-3 and APC Affect Intestinal Cell Number in a CDC-25.1 S46-independent Manner

APC/Axin/GSK3β phosphorylation of the DSG motif of human β-catenin promotes its β-TrCP–dependent degradation (Kikuchi *et al*., 2006), and mutations in APC or the β-catenin DSG motif are associated with human intestinal hyperplasia. To test whether *C. elegans* members of this complex regulate CDC-25.1 through S46, we performed RNAi of candidate genes testing for synergy with the *cdc-25.1(ij48)* mutation. As discussed above, in *C. elegans* the Wnt pathway is required for the specification of the intestinal fate, and similar to previous reports (Rocheleau *et al*., 1997; Schlesinger *et al*., 1999), we observed that RNAi of *gsk-3* or *apr-1*, homologues of GSK3β and APC, respectively, caused a complete lack of intestinal cells in ~18% [*gsk-3(RNAi)*] and ~12% [*apr-1(RNAi)*] of embryos. However, we found the majority of embryos to have more than the normal 20 intestinal cells (Figure 1A and Table 1A). To test whether subsequent to their role in specification of the *C. elegans* intestine, *gsk-3* and *apr-1* have a second function mediated through CDC-25.1 S46 controlling the intestinal cell cycle, we repeated the RNAi in the *cdc-25.1(ij48)* background (Table 1). The number of intestinal cells increased significantly, indicating that *gsk-3* or *apr-1* RNAi is synergistic with *cdc-25.1(ij48)*; and thus, like *pop-1* (see above), do not function through the same pathway as CDC-25.1 S46. Thus, both *gsk-3* and *apr-1* RNAi knockdown can generate extra intestinal cells in a manner distinct from that of *cdc-25(ij48)*. We tested the effect of simultaneous RNAi of *apr-1* and *gsk-3* and found a complete lack of intestinal cells in 20% of embryos, the same as for *gsk-3(RNAi)* alone; hence, no synergy was observed. This is consistent with a model where *apr-1* and *gsk-3* affect intestinal cell number in the same way.

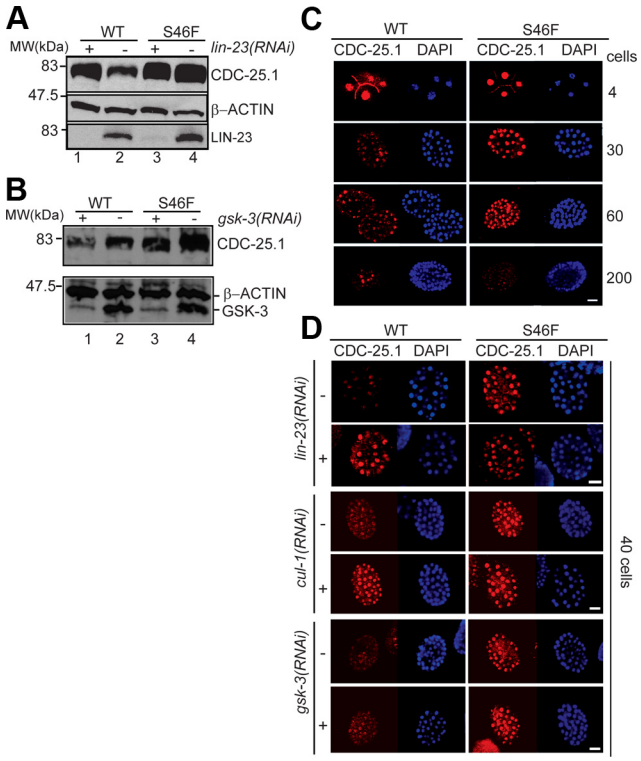

Figure 2. RNAi of *lin-23* and *cul-1* but not *gsk-3* mimic CDC-25.1(S46F) protein increase in all embryonic blast cells. (A) Extracts derived from JR1838 (WT, lanes 1 and 2) or IA530 *cdc-25.1(ij48)* (S46F, lanes 3 and 4) embryos after control (−) or *lin-23(RNAi)* (+) were applied to SDS-PAGE followed by Western blotting against CDC-25.1, LIN-23, or β-actin as loading control. (B) Essentially as in A, but RNAi was performed against *gsk-3* followed by Western blotting against CDC-25.1, GSK3β, and β-actin. (C) Indirect immunostaining of CDC-25.1 (red panels) with corresponding DAPI counterparts (blue panels) in JR1838 (WT) or IA530 *cdc-25.1(ij48)* (S46F) at approximately the 4, 30, 60, or 200 cell stage. Bar, 10 μm. The images shown are representative. Images like these were used in the quantification of intensity of CDC-25.1 immunofluorescence; details of how this was performed are given in the legend to Supplemental Figure 1. (D) Indirect immunostaining of CDC-25.1 (red panels) with corresponding DAPI images (blue channels) in JR1838 (WT) or IA530 *cdc-25.1(ij48)* (S46F) after control, *lin-23*, *cul-1*, or *gsk-3* RNAi. Bars, 10 μm.

LIN-23 Regulates CDC-25.1 Abundance in the Embryo but Not in the Germline

Our genetic data, and those of Hebeisen and Roy (2008), are consistent with the proposal that the CDC-25.1(S46F) protein escapes normal negative regulation by LIN-23. Previously, we detected no difference in abundance between CDC-25.1 and CDC-25.1(S46F) in protein extracts from *C. elegans* adults that contain embryos but where much of the CDC-25.1 protein originates in the adult germline (Clucas *et al*., 2002). We examined CDC-25.1 protein levels specifically in embryonic extracts and detected a substantial increase in CDC-25.1(S46F) abundance compared with the wild type (Figure 2A). To investigate the potential role of LIN-23 in the regulation of CDC-25.1 abundance in the *C. elegans* embryo, we used *lin-23* RNAi on both the wild-type strain and on the *cdc-25.1(ij48)* mutant. *lin-23(RNAi)* resulted in a substantial increase of wild-type CDC-25.1 to a level comparable with that of the CDC-25.1(S46F) mutant but importantly did not cause a further increase in mutant CDC-25.1(S46F) abundance (Figure 2A). From this biochemical evidence, we conclude that LIN-23 negatively regulates CDC-25.1 abundance in the *C. elegans* embryo and that the S46 residue is essential for this normal pattern of regulation. In contrast, *gsk-3(RNAi)* did not increase CDC-25.1 protein levels but in fact resulted in a slight reduction of both CDC-25.1 and CDC-25.1(S46F), whereas the relative elevated abundance of CDC-25.1(S46F) compared with CDC-25.1 remained. Thus, we conclude that GSK-3 is not involved in destabilizing CDC-25.1 via S46 (Figure 2B). The reason for the observed reduction of both CDC-25.1 and CDC-25.1(S46F) abundance with *gsk-3(RNAi)* is unclear, but CDC-25.1 rapidly declines in abundance during early embryogenesis and is not detectable by immunofluorescence by ~3 h after fertilization. *gsk-3(RNAi)* does cause the accumulation of significant numbers of old dying embryos that never hatch, and it is inevitable that the ratio of older-to-younger embryos is altered. This might account for the difference.

The intestinal specific hyperplasia of *cdc-25.1(ij48)* mutants prompted us to test whether CDC-25.1(S46F) protein levels were elevated exclusively in embryonic intestinal cells, although this seemed unlikely due to the substantial difference in abundance observed by Western blots from protein extracts of intact embryos where all tissues are present. As found previously by immunostaining, the abundance of maternally supplied CDC-25.1 in the *C. elegans* embryo rapidly declines during the first few cleavages (Ashcroft *et al*., 1999; Clucas *et al*., 2002; Kostic and Roy, 2002) and with the conditions used here becomes undetectable between the 100- and 200-cell stage. Immunostaining revealed an approximately twofold increase of CDC-25.1(S46F) abundance compared with CDC-25.1 during the 10- to 60-cell stage of embryogenesis in probably all cells (Figure 2C, Table 2, Supplemental Figure S1, and Supplemental Table S2). Details of how we quantified CDC-25.1 immunofluorescence are given in the legend to Supplemental Figure S1.

lin-23(RNAi) increased wild-type CDC-25.1 abundance in all blast cells during the 10- to 60-cell stage in a manner that is indistinguishable from the CDC-25.1(S46F) mutant but did not further increase CDC-25.1(S46F) abundance. Similarly, RNAi of *cul-1* caused an increase in CDC-25.1 but not CDC-25.1(S46F) protein levels. In contrast, *gsk-3(RNAi)* had no effect (Figure 2D, Table 2, Supplemental Figure S1, and Supplemental Table S2). Thus, we conclude that in the wild type, LIN-23 promotes the degradation of CDC-25.1 in all cells of the early *C. elegans* embryo and conversely the CDC-25.1(S46F) mutant is stabilized in all cells of the early embryo.

The evidence presented above suggesting LIN-23–dependent destabilization of CDC-25.1 that is dependent on the presence of S46 caused us to test whether these proteins exist within a complex. We found in embryonic extracts that LIN-23 coimmunoprecipitated with CDC-25.1 (Figure 3) and that relatively more LIN-23 coimmunoprecipitated with wild-type CDC-25.1 than with mutant CDC-25.1(S46F), although CDC-25.1 itself is significantly less abundant than the mutant (Figure 3A). Immunoprecipitated CDC-25.1 was probed with an anti-ubiquitin antibody and a high-molecular-weight smear was detected; this material was not detected in the IgG immunoprecipitation controls, suggesting that it is bound specifically by the anti-CDC-25.1 antibody (Figure 3A). Like LIN-23, this material is less abundant for CDC-25.1(S46F) (Figure 3A), where reciprocally the nonubiquitinated CDC-25.1(S46F) species is more abundant. These data are consistent with a model where LIN-23 targets CDC-25.1 for ubiquitin-mediated proteolysis in the developing embryo, and with CDC-25.1 S46 being important for that regulation. However, with our current biochemical data this

Table 2. Comparative analysis of CDC-25.1 protein levels in the early embryo

	Embryos (JR1838)	WT-fold increase	p value	Embryos (IA530 *cdc-25.1 ij48*)	*ij48*-fold increase	p value
10–20n	22 (3)			22 (3)	1.4	<0.001
30–40n	25 (2)			16 (2)	2.2	<0.001
50–60n	24 (3)			24 (3)	1.9	<0.001
100–200n	19 (3)			19 (3)	1.4	n.s.
lin-23 RNAi 10–20n	15/18 (2)	1.7	<0.001	15/16 (2)	1.1	n.s.
30–40n	19/18 (2)	2.8	<0.001	16/9 (2)	1.0	n.s.
50–60n	13/15 (2)	2.3	<0.001	14/16 (2)	1.0	n.s.
100–200n	10/13 (2)	1.6	<0.01	13/13 (2)	1.0	n.s.
cul-1 RNAi 30–40n	46/39 (3)	2.2	<0.001	40/33 (3)	1.1	n.s.
gsk-3 RNAi 30–40n	56/35 (3)	0.9	n.s.	56/42 (4)	1.1	n.s.

Average -fold increase of CDC-25.1 levels as estimated by immunostaining in embryos of wild-type strain JR1838 compared with IA530 *cdc-25.1(ij48)* (compare WT -fold increase with *ij48*-fold increase). Embryos: number of embryos (number of independent experiments); in RNAi experiments: control RNAi/gene-specific RNAi. p value, two-tailed Student's *t* test, -fold increase was determined as described in Supplemental Table 2. See Supplemental Figure 1 for examples on original data sets and a detailed explanation of how quantification was performed.

model is speculative. The *C. elegans* embryo is impermeable to most drugs; hence, we are unable to block proteasomal degradation to test whether the putative polyubiquinated CDC-25.1 species further accumulates. Likewise, we are unable to block ubiquitination in a manner that would permit biochemical analysis.

CDC-25.1 within the developing embryo is supplied maternally and also is abundant in the maternal germline (Figure 4I) but not in other postembryonic tissues (Ashcroft and Golden, 2002; Clucas *et al*., 2002). By comparing the abundance of CDC-25.1 in embryonic extracts with extracts from late L4 larvae (where the only source of CDC-25.1 is the developing germline), we determined that the S46F mutation does not detectably affect CDC-25.1 abundance in the germline of such animals (Figure 3B). Also, the interaction between LIN-23 and CDC-25.1 is either absent or much reduced in the germline, because LIN-23 did not coimmunoprecipitate efficiently with germline-derived CDC-25.1 (Figure 3C).

However, as detected by immunofluorescence the LIN-23 protein is present both in all blast cells of embryos (Figure 4, A–D) and in the wild-type germline (Figure 4, F,G, H, and J). We find that LIN-23 is present in the germline from the tip of the distal arm to the maturing oocytes (Figure 4F). Its abundance seems relatively similar between the distal and proximal zones; however, its localization is concentrated within cytosol and is relatively excluded from nuclei (Figure 4, F–H and J). The distal region of the gonad is a syncytial tube with the germline nuclei packed around the outside with a hollow core. We find that LIN-23 is concentrated

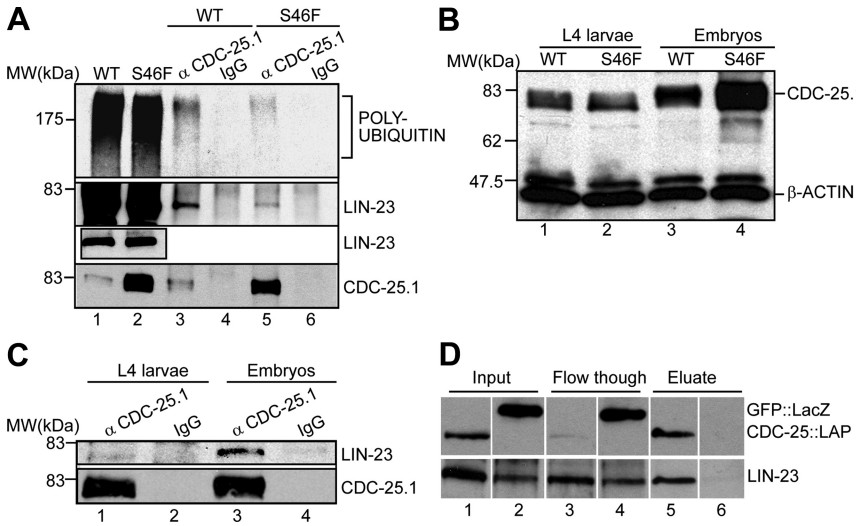

Figure 3. CDC-25.1(S46) is crucial for LIN-23 interaction in *C. elegans* embryos. (A) Immunoprecipitation of CDC-25.1 from *C. elegans* wild-type strain JR1838 (WT, lanes 1, 3, and 4) compared with IA530 *cdc-25.1(ij48)* (S46F, lanes 2, 5, and 6). Samples were precipitated with an anti-CDC-25.1 antibody (lanes 3 and 5) and as control rabbit IgG (lanes 4 and 6). Three percent (9 μg of total protein) of the total fraction were applied to SDS-PAGE for input (lanes 1 and 2) and 30% of the eluates (lanes 3–6), followed by Western blotting and sequential probing with anti-ubiquitin, anti-LIN-23, and anti-CDC-25.1 antibodies. Small inset, weak exposure of input for anti-LIN-23 to show equal protein loading. A typical result obtained from two independent experiments is shown. (B) Comparison of CDC-25.1 protein levels from L4-stage hermaphrodites, mainly expressing CDC-25.1 in the germline (lanes 1 and 2), with the protein levels in the embryo (lanes 3 and 4). Similar amounts of total proteins derived from extracts of JR1838 (WT) and IA530 *cdc-25.1(ij48)* (S46F) were applied to SDS-PAGE, followed by Western blotting with anti-CDC-25.1 and anti-β-ACTIN antibodies, result was obtained from two independent experiments. (C) Immunoprecipitation of CDC-25.1 with the anti-CDC-25.1 antibody (lanes 1 and 3) or as control rabbit IgG (lanes 2 and 4) from extracts derived from L4-stage hermaphrodites (lanes 1 and 2) or embryos (lanes 3 and 4). Eluates were applied to SDS-PAGE followed by Western blotting against LIN-23 and CDC-25.1 (similar to A, two independent experiments). (D) Immunoprecipitation of LAP-tagged CDC-25.1 from embryos. Embryos containing transgenically expressed CDC-25.1::LAP (strain IA535) or as a control GFP::LacZ (strain JR 1838) expressed in intestinal cells were immunoprecipitated with anti S-tag resin. We loaded 1.25% of the total fraction on SDS-PAGE for the input and flow-through (lanes 1–4) and 33% of the total for the eluates (5–6). Western blots were probed with anti-GFP antibodies (top) or anti-LIN-23 antibodies (bottom).

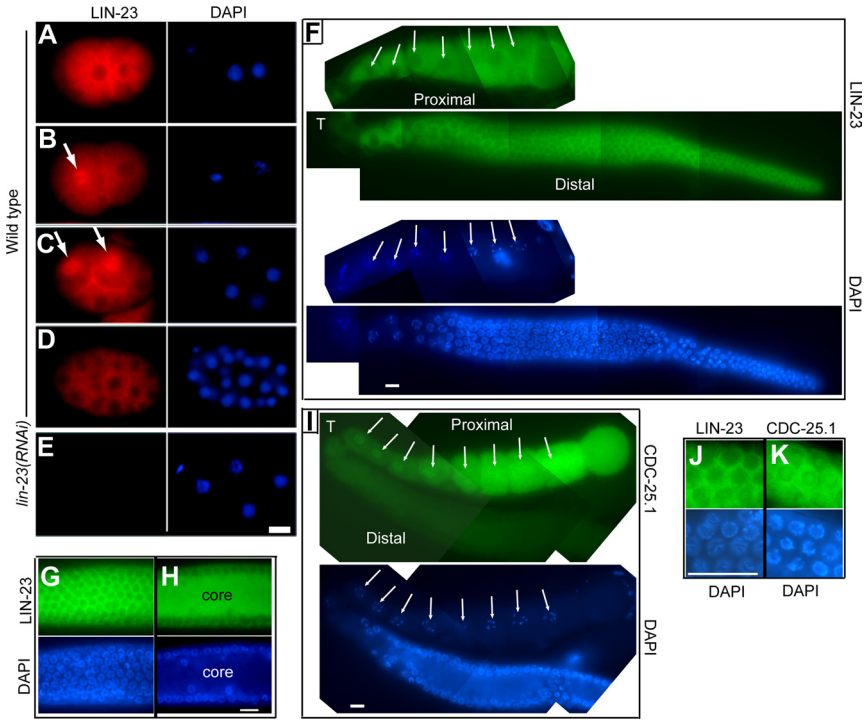

Figure 4. Subcellular distribution of LIN-23 in early embryonic blastomeres and of LIN-23 and CDC-25.1 in adult germline. (A–E) Indirect immunostaining of LIN-23 in wild type (A–D) or *lin-23(RNAi)*–treated embryos (E) by using an anti-LIN-23 antibody (red panels) with corresponding DAPI counterparts (blue panels). Early two-cell embryo (A), late two-cell embryo (B), four-cell embryo (C and E), and 28-cell embryo (D). Nuclear localization of LIN-23 indicated by white arrows in the blastomere AB (B) and ABa and Abp (C). Bar, 10 μm. (F) Indirect immunostaining of LIN-23 in the adult germline of the wild-type strain N2 (green panels) with corresponding DAPI counterparts (blue panels). The position of oocyte nuclei are marked with white arrows and the turn of the gonad labeled with T. The proximal and distal arms of the gonad are labeled and both shown are from the same intact isolated gonad. Bar, 10 μm. (G–H) Indirect immunostaining of LIN-23 in the adult germline of the wild-type strain N2 (green panels) with corresponding DAPI counterparts (blue panels). The section shown is from approximately the middle of the distal arm. The nuclei are packed around the outside of the distal arm, as seen in the top focal plane (G). The core of the distal arm does not contain nuclei, but has strong LIN-23 staining (H). Bar, 10 μm. (I) Indirect immunostaining of CDC-25.1 in the adult germline of the wild-type strain N2 (green panels) with corresponding DAPI counterparts (blue panels). The position of oocyte nuclei are marked with white arrows and the turn of the gonad labeled with T. The proximal and distal arms of the gonad are labeled and are shown in the same orientation as that for F. Bar, 10 μm. (J) Indirect immunostaining of LIN-23 in the adult germline of the wild-type strain N2 (green panels) with corresponding DAPI counterparts (blue panels). The section shown is from approximately the middle of the distal arm similar to the section shown in G, but at higher magnification. Bar, 10 μm. (K) Indirect immunostaining of CDC-25.1 in the adult germline of the wild-type strain N2 (green panels) with corresponding DAPI counterparts (blue panels). The section shown is from approximately the middle of the distal arm similar to the section shown in G, but at higher magnification. Bar, 10 μm.

throughout the core and in the cytosolic spaces between the nuclei and is either absent from, or present at a much reduced level, in the nuclei themselves (Figure 4, G, H, and J). Within developing oocytes in the proximal region of the gonad, it is also more abundant in the cytoplasm than nuclei (Figure 4F).

CDC-25.1 in the germline shows a very obvious gradient of abundance (Figure 4I) being at very low levels in the distal region, becoming obvious in young developing oocytes (toward the top left of the gonad shown) and increasing significantly in more mature oocytes (those toward the top right of the gonad shown). Also, although CDC-25.1 is abundant within the cytoplasm of the oocytes, it is slightly more concentrated within their nuclei (Figure 4I). CDC-25.1 is much less abundant within the distal arm of the gonad (Figure 4I), but extended exposures at high magnification suggest that it is present being located both outside and within the nuclei, but absent from the periphery of nuclei (Figure 4K). By contrast, LIN-23 seems to be absent from these nuclei (Figure 4J). These data demonstrate the progressive accumulation of CDC-25.1 in maturing oocytes and this occurs in the presence of LIN-23.

An interesting observation was the differential localization of LIN-23 in the cells of the early embryo. It is generally distributed throughout the cytosol, but its localization is dynamic being differentially excluded from the nucleus for much of the cell cycle, but a fraction of it accumulates to the nuclear compartment late in the cycle shortly before cell division (Figure 4, A–D). In the embryos shown, the nuclear compartment accumulation of LIN-23 is seen in a late AB blastomere (Figure 4B) but is absent in a slightly younger AB blastomere (Figure 4A). Similarly, it can be seen in both the ABa and ABp blastomeres but absent from the nuclei of the EMS and P2 blastomeres (Figure 4C). Because the ABa and ABp blastomeres divide slightly earlier than EMS and P_2, they are inevitably later in the cell cycle. However, this pattern is not lineage dependent. In other embryos, we have observed localization to a nuclear compartment in EMS and P_2 also. Reminiscent of the behavior of LIN-23 at the two-cell stage, the CDC-25.1 protein has previously been shown to accumulate in the nuclear compartment slightly quicker in the AB blastomere than in P_2, and this is dependent on the function of the PAR proteins (Rivers *et al*., 2008). However, once localized to the nuclear compartment by the late two-cell stage, CDC-25.1 then remains predominantly nuclear throughout most of the cell cycle during the subsequent embryonic stages (Figure 2C; Clucas *et al*., 2002). This contrasts with what is likely to be a more dynamic behavior of LIN-23 which in fixed, stained specimens is more frequently absent from nuclei than CDC-25.1 during later developmental stages (Figure 2, C and D). The dynamic behavior of LIN-23 around the chromatin in early embryonic blastomeres requires further investigation, however, is not observed in the adult germline where it is relatively excluded from the nuclear compartment at all stages (Figure 4, F–H and J).

We were interested to determine whether maternally supplied LIN-23 regulates CDC-25.1 in the embryo. Homozygotes of the null allele *lin-23(e1883)* develop into sterile adults with postembryonic intestinal nuclear division defects as observed previously (Kipreos *et al*., 2000); *lin-*

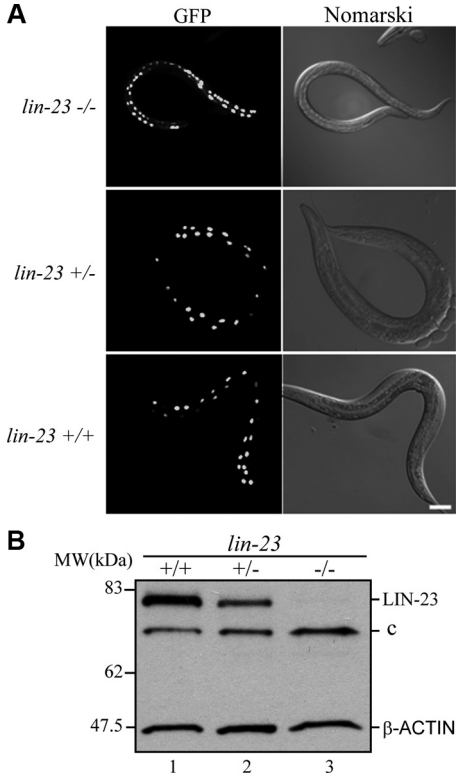

Figure 5. Maternally supplied LIN-23 controls intestinal cell proliferation in the embryo. (A) Offspring derived from *C. elegans* strain IA565 carrying the intestinal-specific GFP marker *npa-1::GFP::LacZ* (see *Materials and Methods* for genotype) was analyzed for the numbers of intestinal nuclei in *lin-23(e1883)* null [*lin-23(−/−)*], *lin-23(e1883)* heterozygotes [*lin-23(+/−)*], or *lin-23* wild type [*lin-23 (+/+)*] hermaphrodites. We were able to confirm the genotype of larvae and embryos using PCR and a restriction site polymorphism between the mutant and wild type. (B) Western blot analysis of LIN-23 protein levels of whole animal lysates of strains analyzed in the top panels. C, cross-reacting band detected with the anti-LIN-23 antibody. A typical result is shown from two independent experiments and several comparative protein loadings.

23(e1883)/+ heterozygotes are phenotypically wild type (Figure 5A). We determined that the heterozygotes have ~50% of the wild-type LIN-23 abundance (Figure 5B); therefore, 50% of normal LIN-23 protein abundance is sufficient for viability and to prevent embryonic intestinal hyperplasia by dysregulation of CDC-25.1. The intestinal cell number was normal in all embryos derived from a heterozygous mother, regardless of their zygotic genotype; therefore, maternal LIN-23 function is sufficient to regulate maternal CDC-25.1 in embryos and to control intestinal cell number during embryonic development. We conclude that the negative regulation of maternally derived CDC-25.1 by maternally derived LIN-23 is developmentally regulated being activated after fertilization in the developing embryo. This is concurrent with the onset of a spatially dynamic behavior of LIN-23 where it periodically accumulates to the nuclear compartment late in the cycle shortly before cell division.

Distinct Functions for LIN-23 in the C. elegans Embryo and Germline

Our investigations detailed above indicate that maternally supplied LIN-23 negatively regulates CDC-25.1 abundance in the embryo but not in the developing germline where both proteins are also present. Here, we find genetic evidence for differences in LIN-23 function between the germline and embryo. We generated a *lin-23::FLAG-TY* epitope-tagged transgene and observed that a chromosomally integrated version of this *lin-23::FLAG-TY (ijIs18)*, was only partially functional. In strains where the only *lin-23* function is provided from *lin-23::FLAG-TY (ijIs18)*, the sterility defect of the *lin-23(e1833)* null mutant is completely rescued (Figure 6A). However, embryos derived from such adults displayed a high frequency (~75%) of embryonic lethality (Figure 6B). Therefore, although *lin-23::FLAG-TY (ijIs18)* completely complements the germline defect of the *lin-23(e1833)* null, it only partially complements its embryonic functions. Also, the viable embryos (and some of the nonviable) displayed an embryonic intestinal hyperplasia (Figure 1A), which we hypothesized might be by a partial failure of S46-mediated regulation of CDC-25.1. Because the *cdc-25.1(ij48)* mutant does not cause embryonic lethality, the lethality associated with the partially functional *lin-23::FLAG-TY (ijIs18)*, must be caused by another mechanism.

To test whether *lin-23::FLAG-TY (ijIs18)* was defective in the regulation of CDC-25.1, we assessed the CDC-25.1 protein levels. CDC-25.1 abundance was elevated in the *lin-23::FLAG-TY* strain to a level similar to that of the mutant CDC-25.1(S46F) in a wild-type *lin-23* background, whereas the abundance of CDC-25.1(S46F) was not altered (Figure 6C). Therefore, the increase in embryonic CDC-25.1 abundance caused by *lin-23::FLAG-TY (ijIs18)* is S46 dependent.

We then tested the physical association of LIN-23::FLAG-TY and CDC-25.1. We found substantially less LIN-23::FLAG-TY than wild-type LIN-23 coimmunoprecipitated with wild-type CDC-25.1 (Figure 6D), although the abundance of CDC-25.1 was elevated and LIN-23::FLAG-TY was similar to endogenous LIN-23 levels. We conclude that the deregulation of CDC-25.1 by *lin-23::FLAG-TY* is via S46 and that the epitope-tagged version of the LIN-23 protein may be less effective at forming a complex with CDC-25.1.

lin-23(RNAi) Causes Hyperplasia of the E Lineage and Fate Transformation in the C Lineage

The developmental fate switch that occurs at the birth of the two sister-cells MS (mesoderm) and E (endoderm) is associated with a concurrent change in the control of the cell cycle in the cell lineages derived from these two blastomeres. The cell cycles of the E cell lineage are notably longer from the point of the birth of the two daughters of E, Ea and Ep (the 2 E-cell stage), compared with the equivalent MS cell lineage (Figure 7A). The switch to the longer cell cycle in the E lineage is thought to be the result of the introduction of a Gap phase in G2 in the intestinal lineage from Ea and Ep (Edgar and McGhee, 1988). Also, to generate precisely 20 intestinal cells from E, the cell cycle terminates in 12 of the cells present at the 16 E cell stage and a fifth cleavage occurs in only four of the 16 E cells (Figure 7A; Sulston *et al*., 1983). By contrast, all of the MS cells undergo a fifth cleavage.

To investigate cell lineage defects caused by *lin-23(RNAi)*, we used four-dimensional microscopic lineage analyses. We used the intestinal marker *elt-2::GFP* to facilitate the identification of cells of the intestinal fate. *lin-23(RNAi*) caused a significant shortening of the endodermal cell cycles from the 4 E cell stage. In the wild type, the times from the second to third, third to fourth, and the fourth to fifth cleavages (from the E blastomere) are ~45, 65, and 130 min, respectively. With *lin-23* RNAi, these are typically shortened to ~35, 55, and 70 min, respectively (Figure 7B), plus *lin-23* RNAi also caused deregulation of cell cycle exit after the fourth cleavage; most intestinal cells undergo prematurely a fifth cleav-

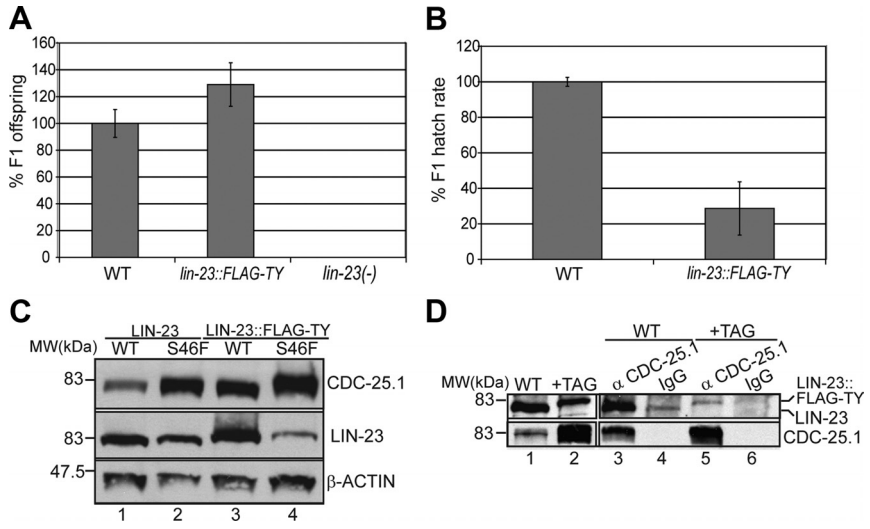

Figure 6. The *lin-23::FLAG-TY* allele rescues germline function of a *lin-23* null mutant but causes embryonic defects. (A) Relative percentage of viable F1 embryos produced by the *C. elegans* strains N2 Bristol (WT), IA589 *lin-23(e1883)* null mutant carrying the *lin-23::FLAG-TY* allele (*lin-23::FLAG-TY*), and the *lin-23(e1883)* null mutant (derived from CB3514). For strain genotypes, see *Materials and Methods*. Mean ± SD, 100 ± 10.4% (WT, three independent experiments), 129 ± 16.3% (*lin-23::FLAG-TY*), and 0% (no viable embryos) [*lin-23(e1883)*], six independent experiments for both. (B) Percentage of hatch rate of N2 Bristol (WT) and IA589 (*lin-23::FLAG-TY*). Mean ± SD (number of embryos in parentheses): 100 ± 2.5% (525) (WT, three experiments), 28.7 ± 15% (1350) (*lin-23::FLAG-TY*, six experiments). (C) Comparison of CDC-25.1 stability in *lin-23* and *lin-23::FLAG-TY* embryos. Equal amount of total protein from embryonic extracts of JR1838 (WT, LIN-23, lane 1), IA530 *cdc-25.1(ij48)* (S46F, LIN-23, lane 2), IA592 (WT, LIN-23::FLAG-TY, lane 3), and IA593 (S46F, LIN-23::FLAG-TY, lane 4) were applied on SDS-polyacrylamide gel and blotted against CDC-25.1, LIN-23, and β-actin. The cause for the low LIN-23::FLAG-TY level in the CDC-25.1(S46F) background is currently unknown. (D) Immunoprecipitation of CDC-25.1 (lanes 3 and 5) compared with control IgG (lanes 4 and 6) from embryonic extracts derived of the strains JR1838 (WT, lanes 1, 3, and 4) or IA592 (+TAG, lanes 2, 5, and 6) a *lin-23* null strain carrying the *lin-23::FLAG-TY* allele (see *Materials and Methods*). Specific copurification of endogenous LIN-23 is observed to endogenous CDC-25.1 but LIN-23::FLAG-TY results in weaker binding to CDC-25.1 (compare lanes 5 and 3). Samples were precipitated with the CDC-25.1 antibody and 3 and 30% of the total fraction applied to SDS-PAGE for input (lanes 1 and 2) and eluates (lanes 3–6), respectively, followed by Western blotting against LIN-23 or CDC-25.1. The presence of the tag in LIN-23 promotes an up-shift of 2.4 kDa in SDS-PAGE.

age (Figure 7B); and in some embryos, we observed a few cells undergo a sixth cleavage (data not shown). Thus, in the E lineage, both the cell cycle length and the decision to exit the cell cycle at the 16 E cell stage are affected by *lin-23* RNAi. The variability of the cell lineage defects seen with *lin-23* RNAi might relate to variation in the extent of interference in different embryos. This interpretation is consistent with the spectrum of outcomes observed, from apparently wild type, through viable with intestinal hyperplasia, to embryonic lethality and the C lineage transformation discussed below. The effects within the E lineage are strikingly similar to those of the *cdc-25.1(ij48)* mutant (Figure 7C; Clucas *et al*., 2002) and to the combination of *lin-23(RNAi*) plus the *cdc-25.1(ij48)* mutant (Figure 7D). In the lineage shown for *lin-23(RNAi)* plus *cdc-25.1(ij48)*, a slightly more severe shortening of the E lineage cell cycles is observed, compared with the *cdc-25.1(ij48)* mutant alone (Figure 7C). Because there is some variability in the E lineage defects for different embryos of both *cdc-25.1(ij48)* mutants and *lin-23(RNAi)*, it is impossible to say whether this apparently minor additive effect is informative or not. In principle, we cannot rule out whether CDC-25.1(S46F) is slightly destabilized by LIN-23 or whether LIN-23 regulates another molecule that has a minor additional effect on the rate of the E lineage cell cycles. It is however possible that this is just an extreme end of the spectra for both *lin-23(RNAi)* and the *cdc-25.1(ij48)* mutant. By contrast, *lin-23(RNAi)* did not cause a shortening of the cell cycles in the MS lineage; and indeed, in the embryo shown there was a slight lengthening of some of the cell cycles from the MSp cell (Figure 7B). This is consistent with *lin-23* and *cdc-25.1* functioning in the same pathway controlling these two aspects of the intestinal lineage; its long cell cycle and the decision to exit the cell cycle after the fourth cleavage and thus determining the cell number of this organ.

We found an additional cell lineage defect in embryos severely affected by *lin-23(RNAi)*, a cell fate transformation in the C lineage where the descendants of Cp (the posterior daughter of C) ectopically adopt the intestinal fate as determined by lineage and expression of the terminal intestinal fate marker *elt-2::GFP* (Figure 7I). In addition, these cells were observed to form a cluster reminiscent of the cell migrations involved in intestinal organogenesis and hence behaved like intestinal cells. Like the intestinal cells derived from the E blastomere with *lin-23(RNAi)* and in the *cdc-25.1(ij48)* mutant, these ectopically derived C lineage intestinal-fate cells display a shorter cell cycle than the wild-type E lineage, and this is not enhanced in the *cdc-25.1(ij48)* background (Figure 7J).

Cell Fate Transformations by gsk-3(RNAi) Demonstrate the Association of Commitment to Intestinal Fate, the Onset of the Long Intestinal Cell Cycles, and Cell Cycle Length Sensitivity to Perturbation of CDC25.1 Regulation

GSK3 affects endodermal fate specification in opposite ways in the E and C lineages such that *gsk-3(RNAi)* causes a transformation within the E lineage to a mesodermal fate and of the Cp lineage to the intestinal fate (Schlesinger *et al*., 1999; Maduro *et al*., 2001). We used these fate transformations to further investigate the relationship between intestinal fate specification, the developmental switch to the longer cell cycle in intestinal cells, and sensitivity of the *C. elegans* embryonic cell cycles to dysregulation of LIN-23–dependent regulation of CDC-25.1. As stated above, we used the intestinal marker *elt-2::GFP* to facilitate the identification of cells of the intestinal fate. We define the cell in which commitment to the intestinal fate occurs as the single progenitor cell of a lineage of cells that all go on to express this marker. Thus, in wild type *C. elegans*, this commitment occurs in the E blastomere where expression of the *elt-2::GFP* marker is first seen two cell divisions later in the 4 granddaughters of E.

Here within the E lineage, *gsk-3(RNAi)* caused a delay in the commitment to and subsequent specification of the intestinal fate. In four of six embryos analyzed, *gsk-3(RNAi)* caused the anterior daughter of E (Ea) to generate nonintestinal cells and the posterior daughter of E (Ep) to produce

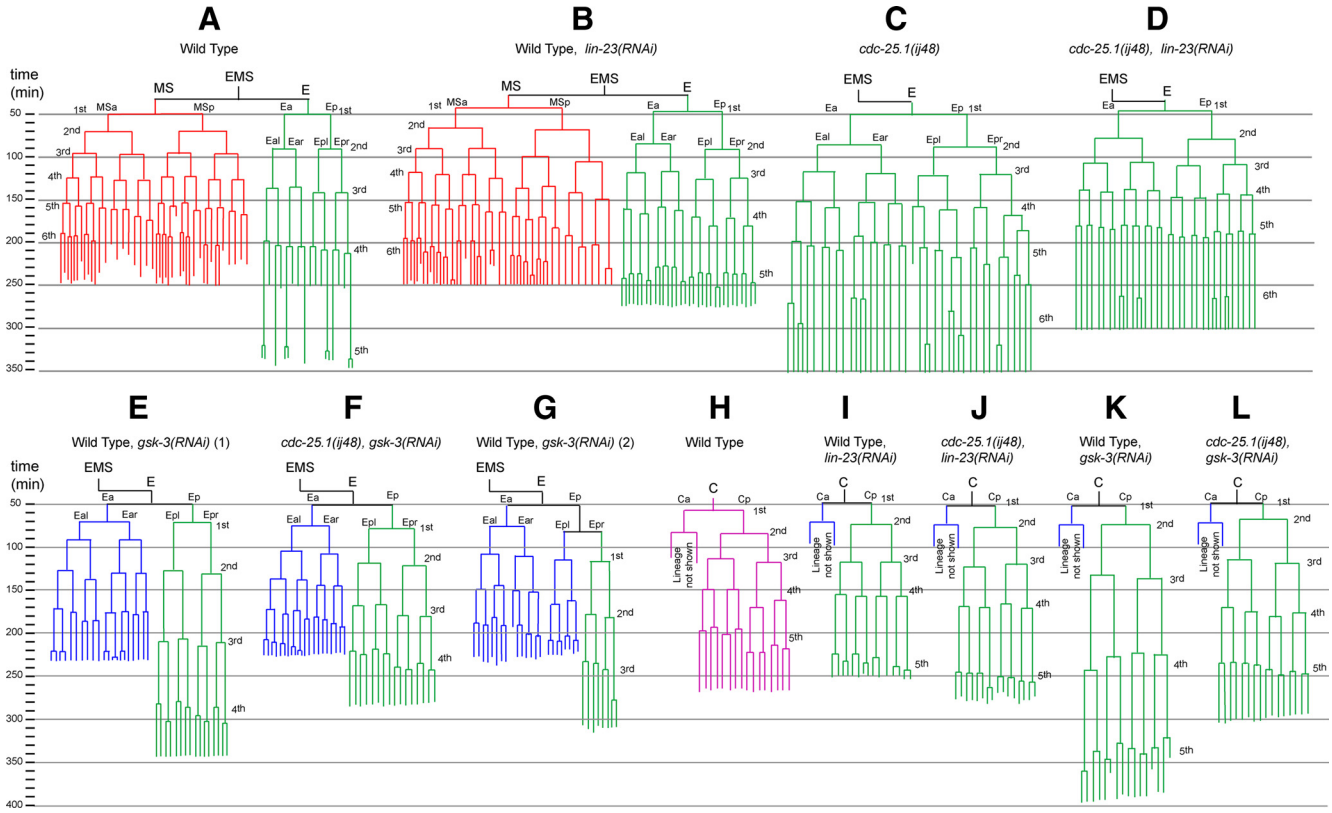

Figure 7. Cell lineage analysis of the E, MS, and C blastomeres. Lineages are derived from wild type or *cdc-25(ij48)* embryos with or without *lin-23* or *gsk-3(RNAi)*, as indicated. The wild-type C blastomere generates ectodermal and mesodermal cells; only Cp is shown. Lineages expressing the intestinal marker *elt-2::GFP* are depicted in green; wild-type MS lineage is in red; wild-type C is in pink; and undetermined but nonintestinal fates in blue. Vertical lines, time between cell divisions; time, minutes post first cleavage. Lineages were followed up to the time indicated by the ends of vertical lines. Lineage analysis was performed on the following: three embryos each for *lin-23* or *gsk-3* RNAi in the wild-type background and *gsk-3(RNAi)* in the *cdc-25.1(ij48)* background and two embryos for *lin-23(RNAi)* in the *cdc-25.1(ij48)* background. For the effect of *lin-23(RNAi)* on the E lineage, those shown are typical, but there is some variability with RNAi. For *gsk-3(RNAi)* on the E lineage, in four embryos analyzed the lineage derived from Ep adopted the intestinal fate, in one embryo the lineage derived from Epr adopted the intestinal fate, and in one embryo the E lineage was wild type. For *gsk-3(RNAi)* on the C lineage, all six embryos analyzed behaved as shown with Cp adopting the intestinal fate. For *lin-23(RNAi)* on the C lineage, ectopic intestinal fate from Cp was observed in two embryos (one of each genotype) and three were wild type. In all cases, the point of specification of the endodermal fate was determined by tracing back to a common ancestor, those cells that at the end of the lineage recordings are determined to express the *elt-2::GFP* marker.

intestine (two embryos shown, Figure 7, E and F); thus, commitment to the intestinal fate is delayed by one cell cycle occurring in the daughter-cell of E, Ep. In one embryo, the intestinal fate commitment was delayed by an additional cell cycle and occurred in Epr (Figure 7G); in one embryo, the E lineage was as wild type (data not shown). In the wild-type E lineage, the switch to the long intestinal cell cycle occurs one division after commitment, the cells Ea and Ep being the first to have a long cell cycle (Figure 7A). Where *gsk-3(RNAi)* delayed commitment to the intestinal fate by one cell cycle occurring in Ep, the switch to the longer intestinal cell cycle was equivalently delayed such that it occurred in Epl and Epr (Figure 7, E and F). Similarly, where commitment occurred two cell cycles late in Epr, the first longer cell cycle was of its daughters Epra and Eprl (Figure 7G). Conversely, those components of the E lineage that with *gsk-3(RNAi)* fail to commit to the intestinal fate (do not give rise to *elt-2::GFP* expression), derived from Ea or from Epl (Figure 7, E and G) display a short cell cycle of very similar length to that of a normal MS lineage (Figure 7A). We examined the sensitivity of *gsk-3(RNAi)* altered E-lineages to the perturbation of LIN-23–dependent regulation of CDC-25.1. When *gsk-3(RNAi)* caused commitment to occur one cell cycle late in Ep in the *cdc-25.1(ij48)* mutant background, the intestinal cell cycles from Epl and Epr onward were shortened compared with the equivalent *gsk-3(RNAi)* in the wild-type background (Figure 7, E and F). However, the short MS-like cell cycles from Eal and Ear are of similar lengths in the wild type and *cdc-25.1(ij48)* backgrounds (Figure 7, E and F) and hence are not sensitive to perturbation of LIN-23–dependent regulation of CDC-25.1.

Similarly, the transformation in cell fate within the C lineage caused by *gsk-3(RNAi)* suggests a stringent association between intestinal-fate specification and sensitivity to CDC-25.1 dysreguation. Here, *gsk-3(RNAi)* promoted ectopic intestinal-fate specification in a proportion of the C lineage with commitment to the intestinal fate occurring in Cp (Figure 7, K and L), the same point as seen above with *lin-23(RNAi)* (Figure 7, I and J). In a wild-type background, this *gsk-3(RNAi)* transformation caused a switch to a typical long intestinal cell cycle one division later in the daughters of Cp (Figure 7K). When performed in the *cdc-25.1(ij48)* mutant background, these intestinal-like cell cycles were shortened (Figure 7L). The combined effect of the *cdc-25.1(ij48)* mutant plus *gsk-3(RNAi)* generates in the lineage from Cp, intestinal-fate cells that have cell cycle lengths

equivalent to the same cells transformed to the intestinal fate by *lin-23(RNAi)* (Figure 7, H and L).

Additional Observations on gsk-3(RNAi) Cell Fate Transformations in the E and C Lineages

We made some additional observations about the fate transformations caused by *gsk-3(RNAi)*. Here, ectopic intestinal fate from Cp was observed in six of six *gsk-3(RNAi)* embryos analyzed (two are shown; Figure 7, K and L), but not in Ca, the anterior daughter of C. Previously, it has been argued C might adopt an EMS-like fate rather than E-like with *gsk-3(RNAi)* (Maduro *et al*., 2001), and our data support that model. The *gsk-3(RNAi)* fate specification defect in the C lineage seems to display polarity. Only the posterior cell touches the embryonic posterior polarity center (blastomere P_2 and descendants) (Schierenberg, 1987; Goldstein, 1995; Thorpe *et al*., 2000; Bischoff and Schnabel, 2006), required to specify the posterior identity (Kaletta *et al*., 1997), which in this case is intestinal identity. Also, in those cases with *gsk-3(RNAi)* where we observed a delay within the E lineage to the commitment to the intestinal fate, occurring in either Ep or Epr, in all cases observed the E-lineage cell where intestinal commitment occurred and its parental cell, were in physical contact with the Wnt-signaling cell P_2, or a descendant of P_2. Hence, the observed polarity of specification may be the result of Wnt signaling. Thus, intestinal fate specification within both the E and C lineages, with *gsk-3(RNAi)*, may be responding to a posterior signal.

In summary, from our cell lineage analysis we propose that *gsk-3(RNAi)* causes a delay in the specification of the intestinal fate within the E-lineage as assessed both by expression of the intestinal-specific marker *elt-2::GFP* and the switch to the long intestinal cell cycle. The longer Gap phase-containing intestinal cell cycles are sensitive to CDC-25.1 activity such that the cell cycles are shortened by the stabilization of CDC-25.1 by perturbation of its LIN-23-dependent regulated degradation. This sensitivity to elevated CDC-25.1 function may be specific to Gap phase containing *C. elegans* embryonic cell cycles because it is not seen in the MS lineage whose cell cycles are short and without an observable Gap phase.

DISCUSSION

In cultured mammalian cells, cell cycle phase-specific fluctuations in the abundance of Cdc25s caused by checkpoint-specific β-TrCP–dependent degradation serve to control cell cycle progression. Here, we demonstrate in the *C. elegans* embryo that LIN-23, the *C. elegans* orthologue of β-TrCP, promotes a gradual decline in the abundance of maternally supplied CDC-25.1 in probably all cells and spanning several embryonic cell cycles, rather than the cyclic pattern for cultured vertebrate cells. Ultimately, this mechanism controls the number of cells in one *C. elegans* organ, the intestine. Because the β-TrCP–dependent degradation of human CDC25A and B occurs via DSG and DDG motifs, respectively (Busino *et al*., 2003; Jin *et al*., 2003), and the CDC-25.1(S46F) mutant that is resistant to LIN-23–dependent degradation is within a DSG motif, we speculate that the molecular mechanism may be conserved between humans and *C. elegans*.

We demonstrated previously by genetic means that *cdc-25.1* function within the embryo is maternal in origin (Clucas *et al*., 2002). Consistent with this, here we demonstrate the presence of the CDC-25.1 protein in the developing *C. elegans* germline, and its progressive accumulation during oocyte maturation. We also demonstrate that the *lin-23* function that promotes the normal degradation of CDC-25.1 in the embryo is maternal in origin and show that the LIN-23 protein is present throughout the adult *C. elegans* germline. Therefore, at the time of fertilization *C. elegans* oocytes contain maternally derived LIN-23 and CDC-25.1 protein synthesized in the germline. During the first few embryonic cell divisions, the CDC-25.1 protein rapidly declines in abundance and becomes undetectable by immunofluorescence between the 100- to 200-cell stage (Clucas *et al*., 2002).

We find several lines of evidence that the relationship between CDC-25.1 and LIN-23 changes between the germline environment and the embryonic environment. The CDC-25.1(S46F) mutant confers stability in the early embryo by escaping LIN-23–dependent degradation causing the mutant protein to be more abundant than the wild type; however, we detected no difference in abundance in protein from the germline. Within the germline, the CDC-25.1 protein accumulates in the presence of LIN-23, being most abundant in the most mature oocytes. This contrasts with the rapid degradation of CDC-25.1 in the embryo. Although we were able to coimmunoprecipitate LIN-23 and CDC-25.1 relatively efficiently from embryonic protein extracts, at best only a trace of LIN-23 was detected by the same method from germline-derived material. The genetic behavior of the epitope-tagged transgene *lin-23::FLAG-TY (ijIs18)* is also pertinent. It rescues completely the germline defect of the *lin-23(e1833)* null mutant by producing normal broods; however, it is significantly defective in embryonic function where, although it is approximately similar in abundance to wild-type LIN-23, it fails to down-regulate CDC-25.1 and also causes ~75% embryonic lethality. Finally, we found that the LIN-23 protein is relatively excluded from nuclei within the germline, but after fertilization its localization is dynamic and it enters the nuclear compartment late in the cell cycle before cell division. Although none of this constitutes proof of the existence of a molecular mechanism that alters the relative behavior of LIN-23 and CDC-25.1 during transit from the germline to embryonic states, in combination these behaviors constitute significant circumstantial evidence that LIN-23 functions differently in the embryo compared with the germline. The postfertilization selective degradation of CDC-25.1 is reminiscent of a variety of *C. elegans* proteins whose degradation is activated during the oocyte to embryo transition by the MBK-2/DYRK kinase (Pellettieri *et al*., 2003). Its targets include OMA-1, also involved in the regulation of the oocyte to embryo transition, and in addition to MBK-2 phosphorylation, timely degradation of OMA-1 also requires the function of the kinases GSK3, CDK-1, and KIN-19 (Shirayama *et al*., 2006). Both MBK-2 and GSK3 have been shown to phosphorylate directly OMA-1 (Nishi and Lin, 2005). Our data suggest GSK3 is not the kinase that targets CDC-25.1 for selective destruction through the DSG motif because unlike OMA-1, *gsk-3(RNAi)* does not stabilize the CDC-25.1 protein; in fact, if anything it reduces its abundance. In addition, LIN-23 itself could be subject to developmental regulation. Our observation that the *lin-23::FLAG-TY (ijIs18)* transgene completely complements the germline defect of the *lin-23(e1833)* null, but only partially complements its embryonic functions, might suggest biochemically distinct functions for LIN-23 in the germline and the embryo. Also, whether the dynamic behavior of LIN-23 in embryonic blastomeres, shuttling between the cytosol and chromatin in a cell cycle dependent manner, relates to its regulated degradation of CDC-25.1 is not known but is certainly worthy of investigation.

CDC-25.1 function is required positively for cell cycle progression in many and possibly all early *C. elegans* embry-

onic cells (Ashcroft *et al*., 1999; Clucas *et al*., 2002; Kostic and Roy, 2002), and LIN-23-regulated decay of CDC-25.1 probably occurs in all early embryonic cells, but hyperplasia by CDC-25.1 stabilization is specific to the intestine. Also, as we show here, because *lin-23(e1883)* homozygous mutants derived from heterozygous mothers have a wild-type number of intestinal cells in the embryo, maternal LIN-23 must be sufficient for adequate regulated degradation of CDC-25.1 in the early embryo; hence, a tissue-specific difference in zygotic *lin-23* expression cannot explain the intestinal specificity of the hyperplasia. A key question therefore is what makes the intestinal cell cycle uniquely sensitive to the abundance of this cell cycle regulator? The early embryonic cell cycles are rapid, consisting simply of S and M phases and the time of introduction of Gap phases varies in different lineages. The first recognized Gap phase is a G2 in the intestinal lineage from Ea and Ep (Edgar and McGhee, 1988), resulting in the lengthening of the intestinal cell cycle (Figure 7A). In addition, a G1 phase at the 16 E cell stage has been proposed, due to the requirement of the G1-type cyclin *cyd-1* for the final intestinal cell divisions (Boxem and van den Heuvel, 2001). Abrogation of LIN-23–dependent degradation of CDC-25.1 in the embryo causes two distinct effects within the intestinal cell lineage; a marked shortening of the intestinal cell cycle and extra rounds of cell division including a fifth cleavage of cells that normally exit the cell cycle after the fourth cleavage, and a sixth cleavage in some cases. Thus, during normal development, CDC-25.1 abundance is rate limiting both with respect to the length of the intestinal cell cycles and also the number of reiterations of the cycle. The progressive regulated degradation of CDC-25.1 ultimately becomes a checkpoint terminating the intestinal cell cycle and regulating the cell number of this single organ. It is probable that the sensitivity of the intestine to CDC-25.1 abundance, and hence the tissue specificity of the phenotype, is linked to the switch to the long intestinal cell cycle and the presence of Gap phases. Interestingly, the cell cycle shortening by stabilization of CDC-25.1 in the *C. elegans* embryo is not entirely restricted to the intestinal lineage. Two other cell cycles are reported to be affected, namely, that of the P_4 blastomere which is significantly shortened, and to a lesser extent that of its sister cell D (Bao *et al*., 2008). Like the intestinal cell cycles, both of these are long by comparison to all other *C. elegans* embryonic cell cycles that occupy a similar position within the cell lineage (the same number of cell divisions from the zygote P_0). Also, the shortening is greater in P_4, which has a longer cell cycle than its sister D. Therefore, CDC-25.1 abundance in the embryo is limiting the cell cycle length of these long cell cycles but not the rapid cell cycles that are believed only to consist of S and M phases.

Interestingly, overexpression of CDC25A and B have been detected in a wide range of human cancers (Kristjansdottir and Rudolph, 2004), and an oncogenic potential has been attributed to CDC25A and B but not C in transformation of murine fibroblasts (Galaktionov *et al*., 1995). Intriguingly, only CDC25A and B are targets of β-TrCP through the DSG/DDG motifs (Busino *et al*., 2003; Jin *et al*., 2003). It would be interesting to know whether the oncogenic potential of CDC25A and B is mediated via loss of their β-TrCP regulation.

An unexpected outcome of this work was the finding of the delay in commitment to the intestinal fate in the E lineage, caused by *gsk-3(RNAi)*. Interpretation of this delay requires consideration of the findings of Schlesinger *et al*. (1999). In the Schlesinger study, laser ablation of all other cells was used to isolate the E blastomere in *gsk-3(RNAi)* embryos and in such 44% failed to generate endoderm. Instead, E seemed to adopt the fate of its sister cell MS as indicated by formation of muscle. Importantly, all isolated E blastomeres that produced mesodermal cells did not produce endodermal cells; a mixture of fates was never observed. That contrasts with our data where we see a mixture, with intestine being produced from Ep but nonintestinal fate cells from Ea. The potentially informative difference is that our results were obtained from the study of lineages within intact embryos; the E blastomeres were isolated in the Schlesinger study and hence allowed to develop in an E cell autonomous manner. In our findings in all cases the E lineage cell where delayed endoderm specification occurred (usually Ep) and its parental cell were in physical contact with a descendant of the Wnt signaling cell P_2, or P_2 itself. Taking our findings and those of Schlesinger together, we suggest that knockdown of *gsk-3* by RNAi can cause a simple E-to-MS fate transformation when the source of the posterior signal is removed, but in intact embryos where the signal persists, it can cause a delay by one or two cell divisions to commitment to the intestinal fate in cells of the E lineage. How might such a delay be generated? The window of time in which the wild-type EMS blastomere and its descendants can respond to the P_2 posterior signal and in which P_2 and its descendants can produce the signal, has been investigated (Goldstein, 1995). In the wild-type embryo, the capacity to respond to the P_2-derived signal persists for only ~6 min in EMS and the daughters of EMS cannot respond. Conversely, the P_2 signal was shown to persist much longer for up to two cell divisions; hence, a source of signal is present later. We suggest that *gsk-3(RNAi)* must cause a delay to the period of responsiveness to the P_2 signal within cells derived from EMS. It would be interesting to determine whether the E blastomere in such cases is truly pluripotent like its normal parent cell EMS and hence if *gsk-3(RNAi)* is promoting a pluripotent state in this lineage.

ACKNOWLEDGMENTS

We thank Jane Shingles and Ian Hope for microparticle bombardment, Richard Wilson for advice with statistical analysis, Iain Cheeseman for technical advice, and Joel Rothman and Morris Maduro for gift of the strains JR1838 and JR667. Some *C. elegans* strains were obtained from the Genetics Stock Center, which is funded by the National Institutes of Health National Center for Research Resources. A. S. was funded by a 4-Year Wellcome Trust prize studentship. Funding for I.L.J. and C. C. was from the Medical Research Council.

REFERENCES

Ashcroft, N., and Golden, A. (2002). CDC-25.1 regulates germline proliferation in *Caenorhabditis elegans*. Genesis *33*, 1–7.

Ashcroft, N. R., Srayko, M., Kosinski, M. E., Mains, P. E., and Golden, A. (1999). RNA-Mediated interference of a cdc25 homolog in *Caenorhabditis elegans* results in defects in the embryonic cortical membrane, meiosis, and mitosis. Dev. Biol. *206*, 15–32.

Bao, Z., Zhao, Z., Boyle, T. J., Murray, J. I., and Waterston, R. H. (2008). Control of cell cycle timing during *C. elegans* embryogenesis. Dev. Biol. *318*, 65–72.

Bei, Y., Hogan, J., Berkowitz, L. A., Soto, M., Rocheleau, C. E., Pang, K. M., Collins, J., and Mello, C. C. (2002). SRC-1 and Wnt signaling act together to specify endoderm and to control cleavage orientation in early *C. elegans* embryos. Dev. Cell *3*, 113–125.

Bischoff, M., and Schnabel, R. (2006). A posterior centre establishes and maintains polarity of the *Caenorhabditis elegans* embryo by a Wnt-dependent relay mechanism. PLoS Biol. *4*, e396.

Boutros, R., Dozier, C., and Ducommun, B. (2006). The when and wheres of CDC25 phosphatases. Curr. Opin. Cell Biol. *18*, 185–191.

Boxem, M., and van den Heuvel, S. (2001). lin-35 Rb and *cki-1* Cip/Kip cooperate in developmental regulation of G1 progression in *C. elegans*. Development *128*, 4349–4359.

Busino, L., Donzelli, M., Chiesa, M., Guardavaccaro, D., Ganoth, D., Dorello, N. V., Hershko, A., Pagano, M., and Draetta, G. F. (2003). Degradation of Cdc25A by β-TrCP during S phase and in response to DNA damage. Nature *426*, 87–91.

Clucas, C., Cabello, J., Bussing, I., Schnabel, R., and Johnstone, I. L. (2002). Oncogenic potential of a *C. elegans cdc-25* gene is demonstrated by a gain-of-function allele. EMBO J. *21*, 665–674.

Desai, A., Rybina, S., Muller-Reichert, T., Shevchenko, A., Shevchenko, A., Hyman, A., and Oegema, K. (2003). KNL-1 directs assembly of the microtubule-binding interface of the kinetochore in *C. elegans*. Genes Dev. *17*, 2421–2435.

Edgar, L. G., and McGhee, J. D. (1988). DNA synthesis and the control of embryonic gene expression in *C. elegans*. Cell *53*, 589–599.

Fire, A., Xu, S., Montgomery, M. K., Kostas, S. A., Driver, S. E., and Mello, C. C. (1998). Potent and specific genetic interference by double-stranded RNA in *Caenorhabditis elegans*. Nature *391*, 806–811.

Fraser, A. G., Kamath, R. S., Zipperlen, P., Martinez-Campos, M., Sohrmann, M., and Ahringer, J. (2000). Functional genomic analysis of *C. elegans* chromosome I by systematic RNA interference. Nature *408*, 325–330.

Galaktionov, K., Lee, A. K., Eckstein, J., Draetta, G., Meckler, J., Loda, M., and Beach, D. (1995). CDC25 phosphatases as potential human oncogenes. Science *269*, 1575–1577.

Goldstein, B. (1993). Establishment of gut fate in the E lineage of *C. elegans*: the roles of lineage-dependent mechanisms and cell interactions. Development *118*, 1267–1277.

Goldstein, B. (1995). An analysis of the response to gut induction in the *C. elegans* embryo. Development *121*, 1227–1236.

Gregorieff, A., and Clevers, H. (2005). Wnt signaling in the intestinal epithelium: from endoderm to cancer. Genes Dev. *19*, 877–890.

Hebeisen, M., and Roy, R. (2008). CDC-25.1 stability is regulated by distinct domains to restrict cell division during embryogenesis in *C. elegans*. Development *135*, 1259–1269.

Jin, J., Shirogane, T., Xu, L., Nalepa, G., Qin, J., Elledge, S. J., and Harper, J. W. (2003). SCFbeta-TRCP links Chk1 signaling to degradation of the Cdc25A protein phosphatase. Genes Dev. *17*, 3062–3074.

Kaletta, T., Schnabel, H., and Schnabel, R. (1997). Binary specification of the embryonic lineage in *Caenorhabditis elegans*. Nature *390*, 294–298.

Kamath, R. S., and Ahringer, J. (2003). Genome-wide RNAi screening in *Caenorhabditis elegans*. Methods RNA Interference *30*, 313–321.

Kikuchi, A., Kishida, S., and Yamamoto, H. (2006). Regulation of Wnt signaling by protein-protein interaction and post-translational modifications. Exp. Mol. Med. *38*, 1–10.

Kipreos, E. T., Gohel, S. P., and Hedgecock, E. M. (2000). The *C. elegans* F-box/WD-repeat protein LIN-23 functions to limit cell division during development. Development *127*, 5071–5082.

Kipreos, E. T., Lander, L. E., Wing, J. P., He, W. W., and Hedgecock, E. M. (1996). cul-1 is required for cell cycle exit in *C. elegans* and identifies a novel gene family. Cell *85*, 829–839.

Korswagen, H. C. (2002). Canonical and non-canonical Wnt signaling pathways in *Caenorhabditis elegans*: variations on a common signaling theme. Bioessays *24*, 801–810.

Kostic, I., and Roy, R. (2002). Organ-specific cell division abnormalities caused by mutation in a general cell cycle regulator in *C. elegans*. Development *129*, 2155–2165.

Kristjansdottir, K., and Rudolph, J. (2004). Cdc25 phosphatases and cancer. Chem. Biol. *11*, 1043–1051.

Lin, R., Hill, R. J., and Priess, J. R. (1998). POP-1 and anterior-posterior fate decisions in *C. elegans* embryos. Cell *92*, 229–239.

Maduro, M. F., Meneghini, M. D., Bowerman, B., Broitman-Maduro, G., and Rothman, J. H. (2001). Restriction of mesendoderm to a single blastomere by the combined action of SKN-1 and a GSK-3beta homolog is mediated by MED-1 and -2 in *C. elegans*. Mol Cell. *7*, 475–485.

Nishi, Y., and Lin, R. (2005). DYRK2 and GSK-3 phosphorylate and promote the timely degradation of OMA-1, a key regulator of the oocyte-to-embryo transition in *C. elegans*. Dev. Biol. *288*, 139–149.

Ougolkov, A., Zhang, B., Yamashita, K., Bilim, V., Mai, M., Fuchs, S. Y., and Minamoto, T. (2004). Associations among beta-TrCP, an E3 ubiquitin ligase receptor, beta-catenin, and NF-kappaB in colorectal cancer. J. Natl. Cancer Inst. *96*, 1161–1170.

Pellettieri, J., Reinke, V., Kim, S. K., and Seydoux, G. (2003). Coordinate activation of maternal protein degradation during the egg-to-embryo transition in *C. elegans*. Dev. Cell *5*, 451–462.

Polakis, P. (2000). Wnt signaling and cancer. Genes Dev. *14*, 1837–1851.

Praitis, V., Casey, E., Collar, D., and Austin, J. (2001). Creation of low-copy integrated transgenic lines in *Caenorhabditis elegans*. Genetics *157*, 1217–1226.

Rivers, D. M., Moreno, S., Abraham, M., and Ahringer, J. (2008). PAR proteins direct asymmetry of the cell cycle regulators Polo-like kinase and Cdc25. J. Cell Biol. *180*, 877–885.

Rocheleau, C. E., Downs, W. D., Lin, R., Wittmann, C., Bei, Y., Cha, Y. H., Ali, M., Priess, J. R., and Mello, C. C. (1997). Wnt signaling and an APC-related gene specify endoderm in early *C. elegans* embryos. Cell *90*, 707–716.

Rocheleau, C. E., Yasuda, J., Shin, T. H., Lin, R., Sawa, H., Okano, H., Priess, J. R., Davis, R. J., and Mello, C. C. (1999). WRM-1 activates the LIT-1 protein kinase to transduce anterior/posterior polarity signals in *C. elegans*. Cell *97*, 717–726.

Schierenberg, E. (1987). Reversal of cellular polarity and early cell-cell interaction in the embryos of *Caenorhabditis elegans*. Dev. Biol. *122*, 452–463.

Schlesinger, A., Shelton, C. A., Maloof, J. N., Meneghini, M., and Bowerman, B. (1999). Wnt pathway components orient a mitotic spindle in the early *Caenorhabditis elegans* embryo without requiring gene transcription in the responding cell. Genes Dev. *13*, 2028–2038.

Schnabel, R., Hutter, H., Moerman, D., and Schnabel, H. (1997). Assessing normal embryogenesis in *Caenorhabditis elegans* using a 4D microscope: variability of development and regional specification. Dev. Biol. *184*, 234–265.

Shirayama, M., Soto, M. C., Ishidate, T., Kim, S., Nakamura, K., Bei, Y., van den Heuvel, S., and Mello, C. C. (2006). The conserved kinases CDK-1, GSK-3, KIN-19, and MBK-2 promote OMA-1 destruction to regulate the Oocyte-to-Embryo transition in *C. elegans*. Curr. Biol. *16*, 47–55.

Sokal, R. R., and Rohlf, F. J. (2000). Miscellaneous methods. Combining probabilities from tests of significance. In: Biometry: The Principles and Practice of Statistics in Biological Research. Vol. 6, ed. R. R. Sokal and F. J. Rohlf, New York, NY: W. H. Freeman and Company, 794–797.

Sulston, J. E., and Hodgkin, J. (1988). Methods. In: The Nematode *Caenorhabditis elegans*, ed. W. B. Wood, Cold Spring Harbor, NY: Cold Spring Harbor Laboratory Press, 587–606.

Sulston, J. E., Schierenberg, E., White, J. G., and Thomson, J. N. (1983). The embryonic cell lineage of the nematode *Caenorhabditis elegans*. Dev. Biol. *100*, 64–119.

Thorpe, C. J., Schlesinger, A., and Bowerman, B. (2000). Wnt signalling in *Caenorhabditis elegans*: regulating repressors and polarizing the cytoskeleton. Trends Cell Biol. *10*, 10–17.

Thorpe, C. J., Schlesinger, A., Carter, J. C., and Bowerman, B. (1997). Wnt signaling polarizes an early *C. elegans* blastomere to distinguish endoderm from mesoderm. Cell *90*, 695–705.

Timmons, L., Court, D. L., and Fire, A. (2001). Ingestion of bacterially expressed dsRNAs can produce specific and potent genetic interference in *Caenorhabditis elegans*. Gene *263*, 103–112.